CHALMERS

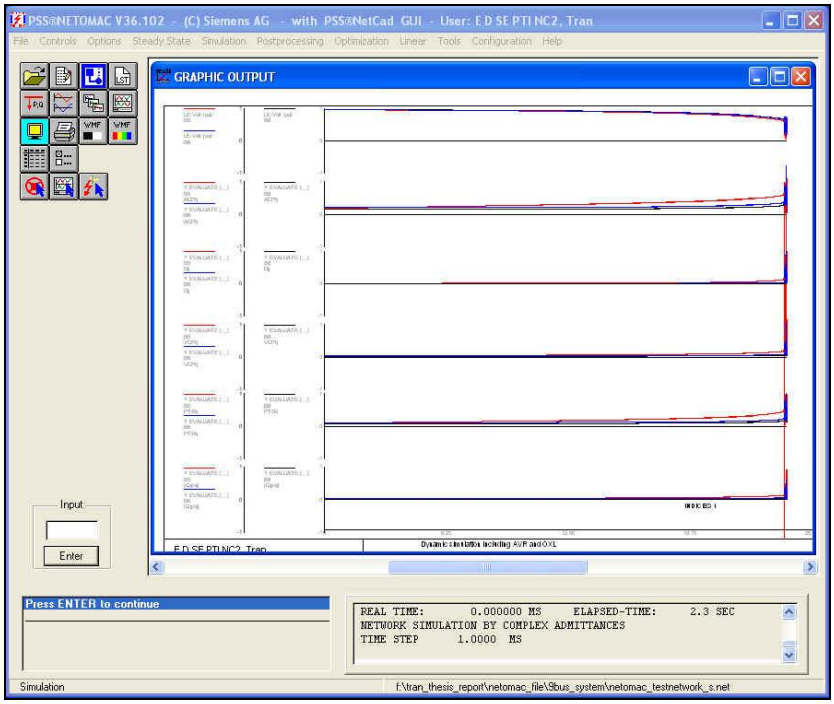

Definition and Implementation of Voltage Stability Indices in PSS®NETOMAC

Master of Science Thesis in Electric Power Engineering

MINH TUAN TRAN

Department of Energy and Environment
Division of Electric Power Engineering
CHALMERS UNIVERSITY OF TECHNOLOGY
Göteborg, Sweden, 2009

Definition and Implementation of Voltage Stability Indices in PSS®NETOMAC

MINH TUAN TRAN

Conducted at Siemens AG
E D SE PTI NC
Erlangen, Germany
Supervisor: Dr. Edwin Lerch
Examiner: Dr. Tuan Anh Le

Department of Energy and Environment
Division of Electric Power Engineering
CHALMERS UNIVERSITY OF TECHNOLOGY
Göteborg, Sweden 2009

Definition and Implementation of Voltage Stability Indices in PSS®NETOMAC

MINH TUAN TRAN

Department of Energy and Environment
Chalmers University of Technology
SE-412 96 Göteborg
Sweden
Telephone + 46 (0)31-772 1000

Göteborg, Sweden 2009

Acknowledgement

I would like to express my thanks to the Swedish Institute, who has given me financial supports during the master program in Sweden.

I am bound to thank my examiner, Dr. Tuan A. Le in Chalmers University of Technology, who has inspired me with his classes and supported me in this thesis topic.

The thesis work is conducted in Siemens AG, Power Technology International, in Erlangen. I am deeply indebted to my supervisor, Dr. Edwin Lerch whose ideals, continuous suggestions and guidance helps me complete the thesis.

My special thanks go to Msc. Tuan N. Trinh, my colleague and dear friend. He has given me valuable supports and encouragements during the time I am doing the thesis.

I also would like to express my thanks to all friends, colleagues in Erlangen, and Göteborg who have given me cheering time and exciting life during the time I am far from home.

Last but not least, I would like to express my gratitude to my family whose patient love enable me to complete this work.

Abstract

This thesis discusses important aspects related to voltage stability indices and their uses in electric power system analysis and operation. Some indices previously studied in the literature are reviewed and implemented in a reduced local network such as Line Stability Index (Lmn), Voltage Collapse Prediction Index (VCPI), and Power Transfer Stability Index (PTSI). In this thesis, a new index, Approximate Collapse Power Index (ACPI), is proposed based on quadratic approximation of PV-curves. All indices are calculated and compared with the existing Siemens's voltage stability criteria, Local Load Index (LLI) and Phase Angle Index (PAI), derived for the reduced local network. The performances of the indices are investigated for both steady-state and dynamic analyses through the IEEE 9-bus test system and a larger test network including 119 generators and 414 nodes using Power System Simulator and Network Torsion Machine Control (PSS®NETOMAC) software. A comparison of the indices regarding to sensitivities, and calculation time has been done. The results show that the performances of these indices are corresponding to one another regarding to voltage stability of the power system. All indices were found falling between 0 and 1 in their intended range. When the system is stable, these indices are closed 0. When the system is in critical condition with regard to voltage instability, the indices moved towards closed to 1, but at different levels of convergence to 1. The Siemens's voltage stability criteria were found less sensitive compared to other indices in the study. They, however, have advantages of shorter calculation time, especially PAI. The proposed ACPI index was found the most sensitive one towards voltage instability. However, ACPI index requires the longest computational time. The ACPI index is recommended to be implemented in the voltage stability assessment module in PSS®NETOMAC.

Key words: Voltage stability, voltage stability indices, P-V curves, dynamic simulations.

Table of Contents

List of Abbreviations

ACPI	Approximate Collapse Power Index
AVR	Auto Voltage Regulator
BCT	Base Calculation Time
ICT	Individual Calculation Time
IEEE	Institute of Electrical and Electronics Engineers
LFF	Load Flow Feasibility
Lmn	Line Stability Index
Nc	Number of Contingencies
NETOMAC	Network Torsion Machine Control
OXL	Over Excitation Limiter
PMU	Phasor Measurement Unit
PSS	Power System Simulator
PTSI	Power Transfer Stability Index
PV	Power Voltage
SSS	Steady State Stability
Tt	Total Simulation Time
VCPI	Voltage Collapse Prediction Index
VS	Voltage Stability

List of Figures

List of Tables

1 Introduction

Recently, several blackouts are reported in many countries relate to voltage stability problems. There are 6 blackouts within 6 weeks in 2003 affecting about 112 million people in US, UK, Denmark, and Sweden [1]. These accidents are due to several common features. They had no problems with generation adequacy, however, all transmission-based. Power systems are operating under increasing stresses. Loads are increasing while transmission networks are not adequately enlarged since economic and environmental restrictions. The power systems are interconnected and they are operated with higher power transfers between areas while there is little coordination and exchange of on-line information between utilities. In essence, the direct cause of blackouts has been found is voltage collapse.

Generally, voltage collapse is the process by which the sequence of events accompanying voltage instability leads to a low unacceptable voltage profile in a significant part of the power system [2]. In power systems, reactive power is needed to support magnetic fields of inductors and electric fields of capacitors in generic loads. The reactive power can be supplied by generators through transmission networks, or compensated directly at load buses by compensators such as shunt capacitors, and synchronous condensers. There are two side effects of reactive power transmission those are transmission losses and voltage drops. When the load voltage is lower, both the transmission losses and voltage drops are higher, which cause the voltage at the load bus more decreased. The voltage constraints prevent long distant transfer of reactive power and the lack of reactive power will directly relate to voltage collapse. It normally follows by a disturbance in the power system. After a disturbance, there is a sudden increase of reactive power demand. If the demand is not met, the disturbance leads to voltage collapse, causing a major breakdown of part or all of the system.

Voltage collapse may be a possible outcome of voltage instability, which is defined as the attempt of load dynamics to restore power consumption beyond the capability of the combined transmission and generation system. [2]. Voltage instability of radial distribution systems has been recognized and understood. It was often referred to as load instability. It may be assessed by the relationship between the voltage and reactive power balance at a load bus. For example if reactive power demand is assumed constant, when the voltage decreases and reactive power supply increase, it is stable. Vice versa, if the voltage decreases together with the reactive power supply it is instable.

There are many affects relating to voltage instability such as dynamic loads, reactive power generations, load tap changer transformers and power transfer capability of transmission systems. Most of these factors have a significant effect on reactive power production, consumption and transmission. Switching of shunt capacitors, blocking of tap-changing transformers, dispatching of generations, rescheduling of generators, secondary voltage regulations, and load shedding, are some of counteractions against voltage collapse.

Researches interested in voltage instability examine two aspects: proximity to voltage instability and mechanism to voltage instability. The first aspect is to determine the current status of power system and estimate the distance to voltage instability by means of physical quantities. The second aspect finds out the reason, contributing factors, involving areas of voltage instability. Proximity

gives a measure of voltage security while mechanism provides information useful in determining activities or operating strategies which could be used to prevent voltage instability [3]

Analysis of voltage instability may be categorized into static and dynamic approaches. In dynamic analysis, all elements of the network are modeled by means of algebraic and differential equations. The study of the power system is done through time domain simulations. The approach requires a lot of computations as well as calculation time. Furthermore, it does not provide readily sensitivity information or the degree of voltage instability. However, it can reflex accurately the mechanism of voltage instability, which in reality a dynamic phenomenon.

The static analysis can be subdivided into Load Flow Feasibility (LFF) and Steady-state Stability (SSS) approaches. These approaches are used to calculate the voltage collapse criteria of the power system. LFF is related to the existence of an acceptable voltage profile across the network based on solving conventional power flow. It is concerned with the maximum power transfer capability of the network or the existence of a solved load flow case based on evaluating the singularity of load flow Jacobian matrix. SSS approach is concerned with the existence of a stable operating point of the power system modeled by algebraic and differential equations. The steady state Jacobian matrix is obtained by solving the set of equations which is linearized around the operating point. This approach evaluates the singularity of the steady state Jacobian matrix to determine the maximum loadability of the power system including affects of generators and other voltage dependent devices [4].

In voltage stability analysis, it is useful to assess voltage stability of power systems by means of scalar magnitudes, or indices. Operators can use voltage stability indices to know how close the system to voltage collapse. These indices may be use on-line or off-line to help operators in real time operation of power system or in designing and planning operations. In literature many static voltage assessment techniques have been proposed, such as the minimum singularity value, mode analysis and sensitivity method [5-7]. The main disadvantages of these techniques include considerable computational efforts making implementation difficult in on-line applications.

Voltage instability often starts in a local network and gradually extends to the whole system. This feature enables to predict static voltage stability using local measurements. There are two types of local evaluation techniques for voltage stability: line-based and node (bus)-based techniques. Conceptually, if a line or a node in the system is critically voltage-instable, the whole system approaches a collapse point [8-11].

The aim of the thesis is to find a voltage stability index which is applicable to be implemented in power system tool PSS®NETOMAC, which is developing by Siemens. The approach of study is to investigate voltage problem of the power system under the feasible solution of load flows of a reduced local network. The voltage stability will be evaluated at each nodes in the system based on the voltages of the node and its surrounding nodes, and the line admittances. In this thesis, some techniques which are based on local phasor measurement will be applied into the reduced local network such as Voltage Collapse Prediction Index (VCPI), Power Transfer Stability Index (PTSI). Line Stability Index (Lmn). Besides, a new index, Approximate Collapse Power Index (ACPI) based on quadratic approximation of PV- curves is proposed. These indices then are compared with Siemens specific voltage stability criteria, Local Load Index (LLI), and Phase Angle Index (PAI) regarding to sensitivities and calculation time. The performances of these indices are verified through static and dynamic analysis of a 9 bus test system and a larger test network including 414 buses and 119 generators.

The analyses presented in this thesis are developed using the software tool and acknowledgments from Siemens AG, Power Technology International (Siemens PTI) department in Erlangen, Germany. The contribution of this work for the company involves the necessity to implement a

meaningful voltage stability index in a voltage stability module in power system simulator PSS®NETOMAC.

The structure of the thesis is as followings:

- Chapter 1 (this chapter) gives backgrounds and objectives of the thesis
- Chapter 2 introduces definitions of voltage stability, the approach to study voltage stability. Infinite-bus system is introduced to evaporate the basic concept in voltage stability. A short description of simulation tool PSS®NETTOMAC is presented.
- Chapter 3 reviews some earlier indices of voltage stability including PV, and QV curve, some indices based on different deriving methods refer to local phasor measurements.
- Chapter 4 introduces a reduced local network. Siemens voltage criteria and a new voltage stability index are derived. Indices reviewed in chapter 2 are implemented in the local network. This section also sets up calculating the indices in PSS®NETOMAC
- Chapter 5 investigates the performance of the indices in test networks. The study is conducted in both static and dynamic approaches with different scenarios. Performance of the indices regarding to sensitivities, and calculation time are compared.
- Chapter 6 summaries the performance of the indices and give some discussions and conclusions.

2 Voltage Stability

Voltage stability is a problem in power system which is lack of reactive power support when heavily loaded or the network transfer capability is reduced due to disturbances. The problem of voltage stability concerns the whole power system, although it usually has a large involvement in one critical area of the power system.

This chapter describes some basic concepts of voltage stability. First voltage stability, voltage instability and voltage collapse are defined. Infinite-bus system is introduced to present PV curve and maximum power transfer. Then different methods of voltage stability analysis are briefly introduced. A short introduction of simulation tool PSS®NETOMAC is presented.

2.1 Concept and classification of voltage stability

Beside rotor angle stability, or transient stability, power system stability also concerns to voltage stability. In [12], the voltage stability is defined as follows: "The voltage stability is the ability of a power system to maintain steady acceptable voltages at all buses in the system at normal operating conditions and after being subjected to a disturbance."

According to [2] the definition of voltage instability is "Voltage instability stems from the attempt of load dynamics to restore power consumption beyond the capability of the combined transmission and generation system."

Voltage instability may, or may not lead to voltage collapse, which is defined by [2] as the catastrophic result of a sequence of events leading to a low-voltage profile suddenly in a major part of the power system. When lacking of the reactive power transfer capability to the load, the power system may cause voltage instability. Therefore, any changes in the power system which affects the reactive power transfer such as dynamic loads, reactive power generation, disconnection of transmission lines, or switching off static compensators are factors relating to voltage instability.

Classification of voltage stability helps analysis the problem, and identifies factors relating to voltage instability. Depending on time scale, Voltage stability is classified as short term and long term voltage stability. Short term voltage stability involves dynamics of fast acting load components like induction motors, electronically controller loads. The study period of interest is in order of several seconds. While long term voltage stability refers to slower acting equipments like tap changing transformers, generator current limiters. The study period of interest extends to several minutes [12]

2.2 Analysis of voltage stability

2.2.1 Single load, infinite bus system

The characteristics of voltage stability are illustrated by an infinite-bus system. In figure 2.1, infinite bus has constant voltage, E. The load is assumed have constant power factor $\cos\phi$. The line impedance is $\underline{Z}$=R+jX.

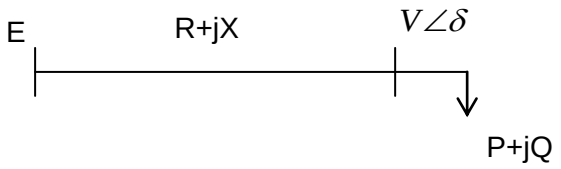

Figure 2.1 Single load, infinite-bus system

The purpose is to calculate the load voltage *V* with different values of load. The voltage is calculated by solving the load flow equation:

$$\frac{\underline{V}^{*}.(\underline{E}-\underline{V})}{\underline{Z}} = \underline{S}^{*} \tag{2.1}$$

where, E is the voltage at the infinite bus , E = E

V is the voltage at the load, V= $V\angle\delta$

S is the load power demand S = P+jQ

Z is the line impedance, Z = R+ jX

Solving equation 2.1 for the load voltage by eliminating the voltage angle, if assuming lossless line, or R=0 it is obtained as follows:

$$V = \sqrt{\frac{E^2}{2} - QX \pm \sqrt{\frac{E^4}{4} - X^2P^2 - XE^2Q}} \tag{2.2}$$

The solutions of load voltages are often presented as a PV-curve as show in figure 2.2.

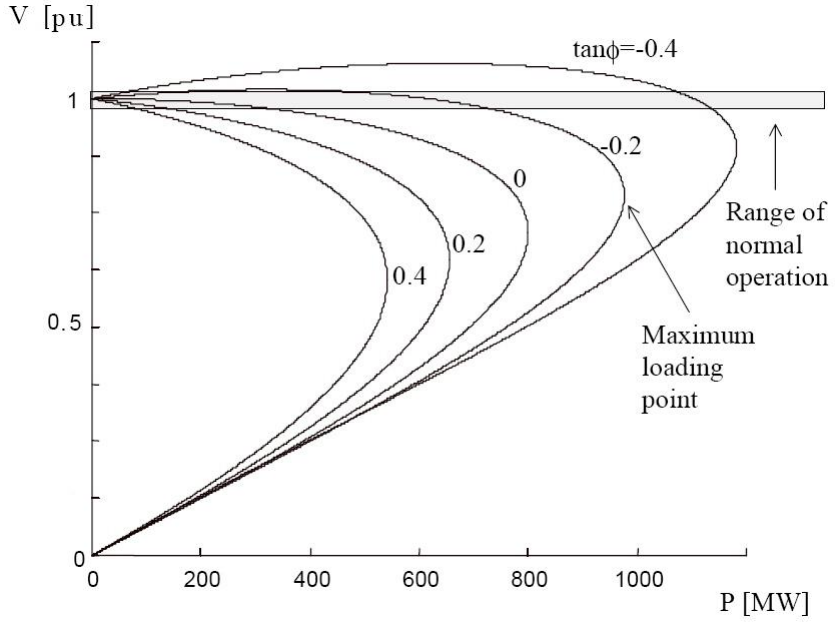

Figure 2.2 PV curves for different load power factors

Figure 2.2 illustrates PV- curves for different load power factors. For each curve, it presents both solutions of power system. The higher voltage solution, which is corresponding to "+" sign in equation 2.2 is stable, while the lower voltage, corresponding to "-" sign, is unstable. In normal operation, power systems are operated in the upper part of the PV-curve. The head of the curve is called the maximum power point where solutions unite [2]. The maximum power and the voltage of the point are obtained when impedance of the load is equal with impedance of the transmission line. They are calculated as follows:

$$P_{\max} = \frac{\cos\phi}{1+\sin\phi}\frac{E^2}{2X} \quad (2.3)$$

$$V_{\max P} = \frac{E}{\sqrt{2}\sqrt{1+\sin\phi}} \quad (2.4)$$

where, $\cos\phi$ is the load power factor which can be calculated as:

$$\cos\phi = \frac{P}{\sqrt{P^2+Q^2}} \quad (2.5)$$

PV-curves play a major role in understanding and explaining voltage stability. From a PV curve, the variation of bus voltages with load, distance to instability (VS margin) and critical voltage at which instability occurs may be determined [13]

2.2.2 Voltage stability analysis in nonlinear power systems

Voltage instability is a dynamic phenomenon which may involve the interaction of many devices. It may occur in different time frames and involve different parts of the system with nonlinear behaviours due to interaction of different elements in power systems. Analysis of voltage stability must provide information on system state, proximity to, and mechanism of instability [13]. There are two main methods of voltage stability analysis in nonlinear power systems: dynamic analysis and static analysis.

2.2.2.1 Dynamic analysis

In dynamic analysis, all elements in a power system are modelled by algebraic and differential equations. The behaviour of the system under different changes of the system is studied through time domain simulations. The whole power system can be expressed under set of algebraic and differential equations in general form as follows:

$$\frac{dx}{dt} = f(x, y, p) \quad (2.6)$$

$$0 = g(x, y, p) \quad (2.7)$$

with a set of know initial condition (x_0,y_0,p_0), where:

x is the state vector of the system (e.g., generator phase angle and angular velocities, tap ratio of on-load tap changer transformers)

y is the vector of algebraic variables (e.g., the direct and quadrature axis components of the stator currents)

p is the vector of parameter variables (e.g., load factor)

For a fix parameter p, equations (2.6), (2.7) are solved directly in time domain by using numerical integration methods such as Euler, Range-Kutta methods [13]. Dynamic analysis can accurately replicate the actual dynamic of voltage stability, and show performance of system and individual elements. It can also capture the event and chronology leading to voltage instability. However, this method requires huge data information for modelling and expensive calculation efforts, while the degree of instability is not provided [3]. In practice, dynamic simulation is applied in essential studies relating to coordination of protections and controls and short-term voltage stability analysis.

2.2.2.2 Static analysis

2.2.2.2.1. Steady-state stability

Steady-state stability approach investigates the power system around each operating point, which is approximated by setting the time derivatives of state variables to zero, and the state variables take on values appropriate to the operating point. Consequently, the overall system equations reduce to purely algebraic equations:

$$0 = f(x, y, p) \quad (2.8)$$

$$0 = g(x, y, p) \tag{2.9}$$

The nonlinear algebraic equations (2.8), (2.9) are linearized around the operating point. It is presented in general form as follows:

$$\begin{bmatrix} \Delta \dfrac{dx}{dt} \\ 0 \end{bmatrix} = J \begin{bmatrix} \Delta x \\ \Delta y \end{bmatrix} \tag{2.10}$$

where, J is the unreduced Jacobian matrix of the system:

$$J = \begin{bmatrix} f_x & f_y \\ g_x & g_y \end{bmatrix} \tag{2.11}$$

where, f_x, f_y are partial derivatives of f(x,y,p) to x, y respectively

g_x,g_y are partial derivatives of f(x,y,p) to x, y respectively.

If assuming that g_y is non-singular Δy can be eliminated from (2.10):

$$\Delta \frac{dx}{dt} = F_x \Delta x \tag{2.12}$$

where, F_x is the reduced Jacobian matrix of the system:

$$F_x = \left[f_x - f_y g_y^{-1} g_x \right] \tag{2.13}$$

The stability of an equilibrium point of the system depends on the eigenvalues of the reduced Jacobian matrix. If all the eigenvalue of this matrix have negative real parts, the operating point is asymptotically stable. If at least one eigenvalue has a positive real part, the operating point is unstable [2]

2.2.2.2.2. Load flow feasibility

The load flow feasibility approach is concerned with the existence of a solved load flow case. The power flow equations for any node k in the power system can be written in real form as follows [13]:

$$P_k = V_k \sum_{m=1}^{n} (G_{km} V_m \cos\theta_{km} + B_{km} V_m \sin\theta_{km}) \tag{2.14}$$

$$Q_k = V_k \sum_{m=1}^{n} (G_{km} V_m \sin\theta_{km} - B_{km} V_m \cos\theta_{km}) \tag{2.15}$$

where, P_k, Q_k are active and reactive power injecting into node k respectively

V_k, V_m are voltage magnitude at node k, and node m respectively

$G_{km} + jB_{km}$ is mutual admittance between node k and node m ($m \neq k$)

= negative of sum of all admittance between node k and node m

$G_{kk} + jB_{kk}$ is self admittance at node k

= sum of all admittance terminating at node k

θ_{km} is the voltage angle difference between node k and node m

Powers at a node is a function of voltage magnitudes and angles at all nodes. Application of Newton-Raphson method, relation of power mismatches with voltage magnitude and voltage angle mismatches are presented as follows:

$$\begin{bmatrix} \Delta P \\ \Delta Q \end{bmatrix} = \begin{bmatrix} \dfrac{\partial P}{\partial \theta} & \dfrac{\partial P}{\partial V} \\ \dfrac{\partial Q}{\partial \theta} & \dfrac{\partial Q}{\partial V} \end{bmatrix} \begin{bmatrix} \Delta \theta \\ \Delta V \end{bmatrix} \tag{2.16}$$

where, $\begin{bmatrix} \dfrac{\partial P}{\partial \theta} & \dfrac{\partial P}{\partial V} \\ \dfrac{\partial Q}{\partial \theta} & \dfrac{\partial Q}{\partial V} \end{bmatrix}$ is the power flow Jacobian matrix.

Equation (2.16) is written for all PQ nodes. For PV nodes where P and V are specified ΔP, ΔQ should be eliminated. Therefore, the Jacobian matrix would have one row and column for each PV node.

The load flow feasibility approach determines the power system conditions for existing solutions of equation (2.16). The method evaluates the power flow Jacobian matrix which should not be singular to achieve a solution for power flow in the power system.

Static analysis offers several advantages. It can provide insight into state, proximity to, and mechanism of instability. Furthermore, modelling assumption helps the calculation time reduced compared to dynamic approach. However, it does not give information if the operating point can be reached and unable to applied in short term voltage stability. In practice, static analysis is used for bulk of planning and operating studies where many contingencies must be analyzed. Besides, the approach is applied in real time operation of power system where fast calculation time is necessary [3].

2.2.3 Introduction of simulation software PSS®NETOMAC

PSS®NETOMAC (Power System Simulator and Network Torsion Machine Control) is a program researched and developed by Siemens. It performs calculations relating to electrical systems consisting of a network, machines and open-loop and closed-loop control equipments [14]. The software has a uniform database and enables the following calculations:

- Simulation of electromagnetic and electro-mechanic transient phenomena in the time domain
- Calculation of instantaneous values with simulation of the network and machines by means of differential equations. Calculation of stability with simulation of the network using complex impedance and machines by means of differential equations
- Special calculations of load flow
- Frequency domain analysis
- Eigenvalue analyses
- Simulation of torsional oscillation systems
- Parameter identification
- Optimization
- Reduction of passive networks

With PSS® NETOMAC, differential-equation systems of electrical systems are integrated step by step. In the analyses of both time and frequency domain as well as eigenvalue analyses, the load-flow program can be used to determine the working point. The possible ways of simulation are shown in figure 2.3.

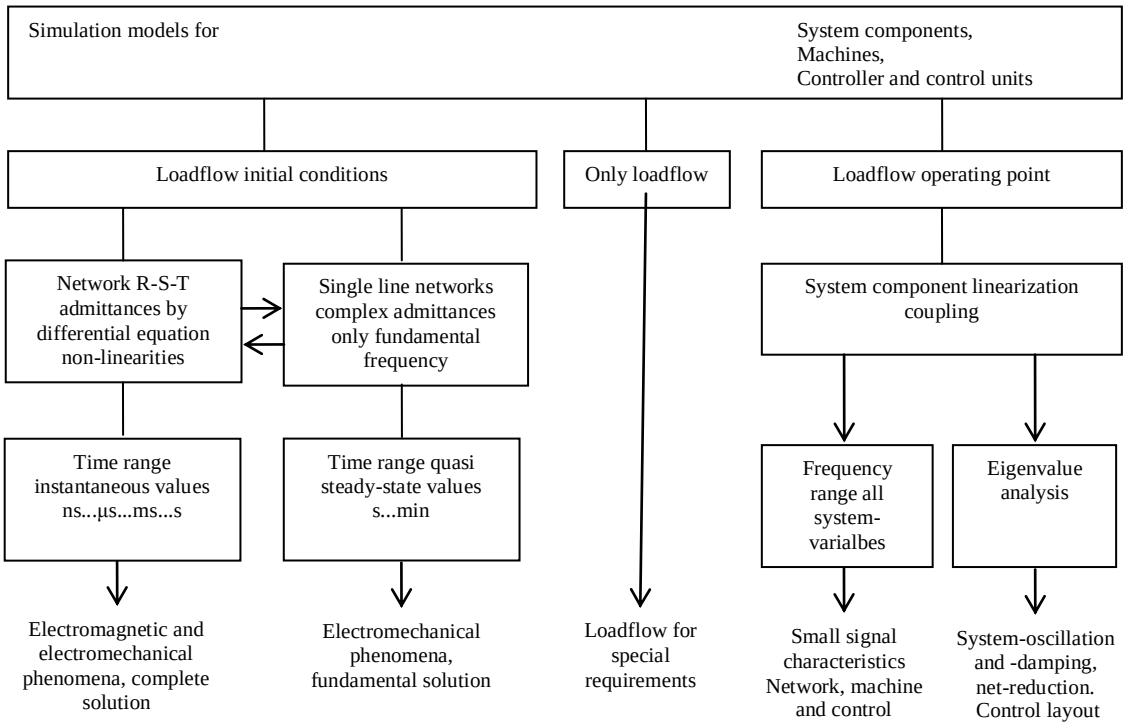

Figure 2.3 Possible ways of simulations

When PSS® NETOMAC is used in parameter identification and optimization it is called as a subroutine. The relationship is shown in figure 2.4.

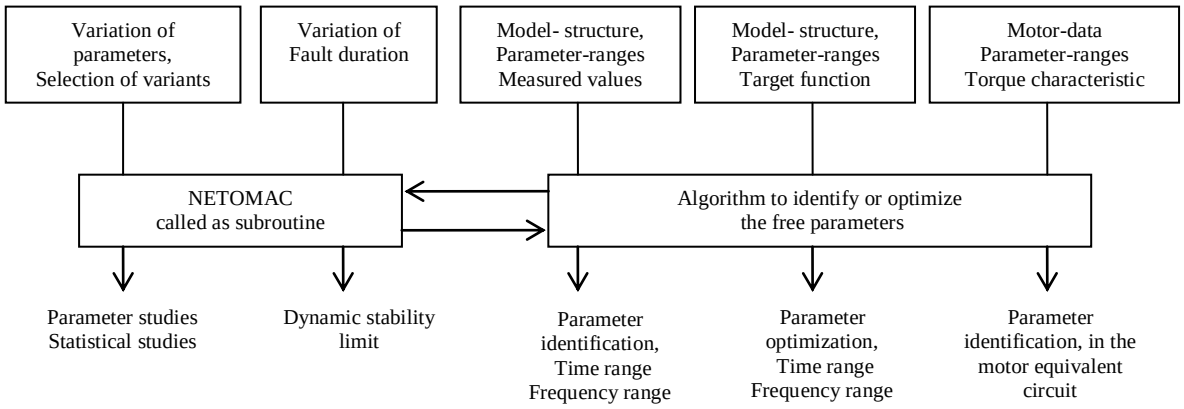

Figure 2.4 PSS® NETOMAC as subroutines for identification and optimization

There are some main characteristics of PSS®NETOMAC:

- Using only one input data file to do all calculations.
- Flexible uses of variables help the input data file easier to be read and modified
- Controller design is a very important characteristic. A block-oriented language is adopted to design controllers.
- Ability to use variant calculations, which facilitate looped simulations
- Parameter setting of simulation data, output data can be implemented and modified online

3 Voltage Stability Indices

In voltage stability analysis, it is interesting and useful to know as the system parameters change prone to voltage stability by mean of monitoring scalar magnitudes, or indices. Operators can use the indices to know how close the system to voltage collapse, or how much power that the system can supply to loads. These indices should be use on-line or off-line to help operators in real time operation of power system or in designing and planning operations. These indices should have a predictable shape, linear, and sensitive with the system change relating to voltage problem so that acceptable prediction can be made and necessary activities can be activated to mitigate the problem. Furthermore, they should be simple, easy to implement and computationally inexpensive, particularly for on-line system monitoring [15]

The condition of voltage stability in a power system can be known using voltage stability indices. These indices may be based on static analysis or dynamic models of the power systems. They can either reveal the critical bus of a power system or the stability of each line connected between two buses in an interconnected network or evaluate the voltage stability margins of a system. In literature, many techniques that approximate voltage collapse based on LFF and SSS approaches have been developed such as PV and QV curves, modal analysis [6], sensitive method [16], voltage phasor approach [17], eigenvalue method [5]. This section reviews some voltage collapse criteria which is capable to be applied in a reduced local network, which is introduced in section 4, and simple to be implemented in PSS®NETOMAC software.

3.1 Loading margin

Loading Margin is the most basic and widely accepted method to approximate voltage collapse in the power system. For a current operating point, the total of increment of load in a specified pattern of load increase that would cause a voltage collapse is called the loading margin to voltage collapse. [15]

The PV and QV curves are the most used to determine the loading margin of a power system at an individual load bus. A typical PV curve of a load bus in the power system is shown in figure 3.1. To build the PV curve, at a base case, the power system load is gradually increased. For each incremental load, it is necessary to recalculate power flows so that the bus voltage corresponding to the load is determined. The increment of load is stopped when the voltage collapse point or the nose of the PV curve is reached. The power margin between the current operating point and the voltage collapse operating point is used as a voltage stability criterion

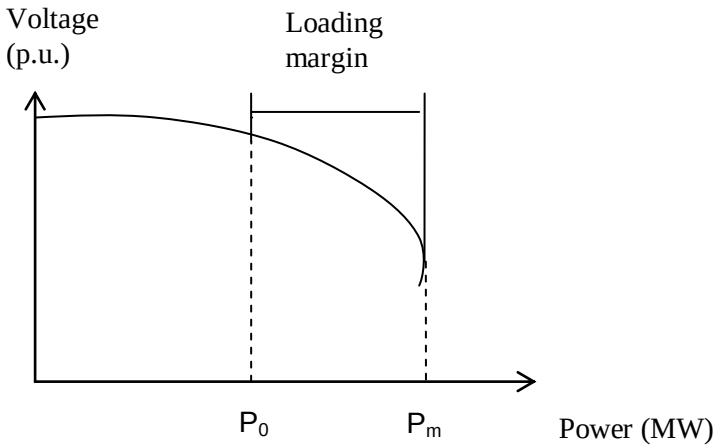

Figure 3.1 PV curve of a load bus in the power system

In figure 3.1, P_0 is the load power at the current operating point, and P_m is the maximum active power that the load can consume from the system.

With Q-V curve, it is possible to know the maximum reactive power that can be achieved or added to a bus before reaching the minimum voltage limit. A typical QV curve is presented as in figure 3.2. The curve can be produced by varying the reactive power demand (or injection) at the load bus while maintaining the active power constant, corresponding load voltage is determined through load flow recalculation. The reactive power margin is the MVar distance from the operating point to the bottom of the Q-V curve. The Q-V curve can be used as an index for voltage instability. The point where dQ/dV is zero is the point of voltage instability.

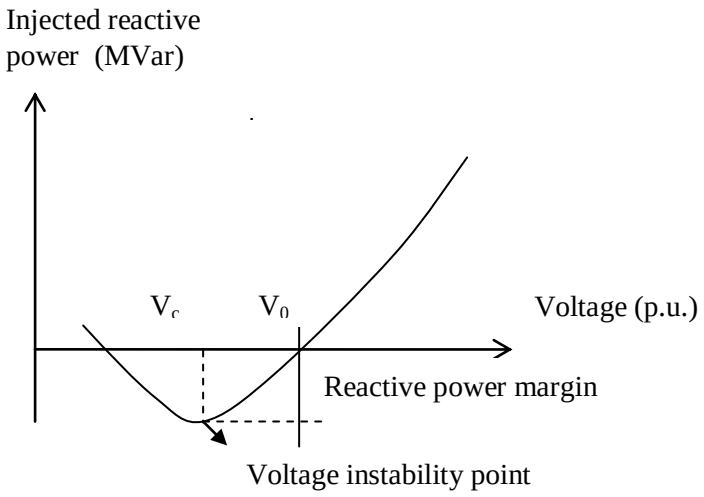

Figure 3.2 QV curve of a load bus in the power system

In figure 3.2, V_0 is the voltage at the load bus at the current operating point. V_c is the voltage at the bottom of Q-V curve, which is the minimum voltage limit within stability of the system.

Generally such curves are developed by load flow analysis, using conventional, direct, and continuation power flow methods [15]. The advantage of the loading margin approach is simple and easy to understand. The procedure of building these curves can be automated. However, the curves

must be generated at each bus. Furthermore, it needs information of the system which is beyond the operating point hence the cost of calculations will be very high.

3.2 Line stability index

M. Moghavemmi et al. [9] formulated a line stability index based on the power transmission concept in a single line, in which the discriminator of the voltage quadratic equation is set to be greater or equal than zero to maintain stability. Figure 3.3 illustrates a single line of an interconnected network where the index is derived from.

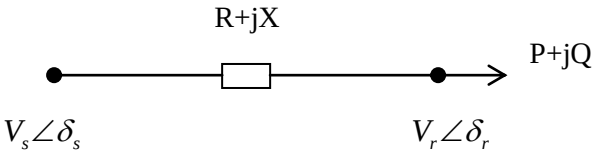

Figure 3.3 Single line diagram of a transmission line in the power system

The line stability index, for this model, can be defined as:

$$Lmn = \frac{4XQ}{[V_s \sin(\theta - \delta)]^2} \tag{3.1}$$

where, $V_s\angle\delta_s$, $V_r\angle\delta_r$ are the sending end and receiving end voltages

R+jX is the impedance of the transmission line

P+jQ is the receiving end apparent power

θ is the line impedance angle

δ is the angle difference between the supply voltage and the receiving end voltage.

Lmn calls the stability index of that line. It is used to find the stability index for each line connected between two bus bars in an interconnected network. Based on the stability indices of lines, voltage collapse can be predicted. When the stability index Lmn less than 1, the system is stable and when this index exceeds the value 1, the whole system loses its stability and voltage collapse occurs.

3.3 Voltage collapse prediction index

Balamourougan et al. [10] proposed a voltage stability index based on the voltage phasor information of the participating buses in the system and the network admittance matrix. Using the measured voltage phasor and the network admittance matrix of the system, the voltage collapse prediction index (VCPI) is calculated at every bus. The value of the index determines the proximity to voltage collapse at a bus.

The technique is derived from the basic power flow equation, which is applicable for any number of buses in a system. The power flow equations are solved by Newton Raphson method, which creates a partial matrix. By setting the determinant of the matrix to zero, the index at bus k is written as follows:

$$VCPI_k = \left| 1 - \frac{\sum_{m=1, m\neq k}^{N} V_m^{'}}{V_k} \right| \tag{3.2}$$

where, $V_m^{'} = \frac{Y_{km}}{\sum_{j=1, j\neq k}^{N} Y_{kj}} V_m$ (3.3)

V_k is the voltage phasor at bus k
V_m is the voltage phasor at bus m
Y_{km} is the admittance between bus k and m
Y_{kj} is the admittance between bus k and j
k is the monitoring bus
m is the other bus connected to bus k
N is the bus set of the system.

The value of VCPI varies between 0 and 1. If the index is zero, the voltage at bus k is considered stable and if the index is unity, a voltage collapse is said to occur. VCPI is calculated only with information of voltage phasor of participating buses and impedance of relating lines. The calculation is simple without matrix conversion. The technique offers fast calculation which can be applied for online monitoring of the power system.

3.4 Power transfer stability index

Nizam et al. [18] derived the power transfer stability index (PTSI) by considering a simple two-bus Thevenin equivalent system, with a slack bus connected to a load bus by a single branch as shown in figure 3.4.

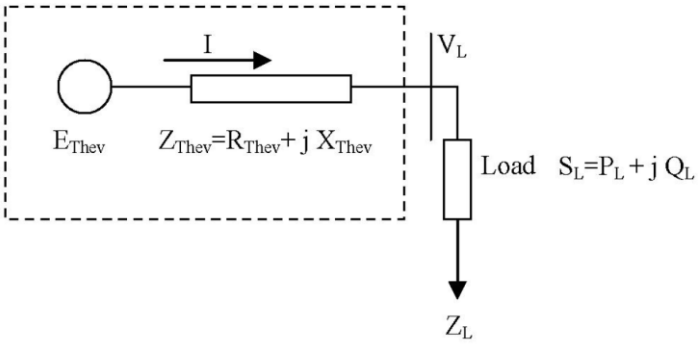

Figure 3.4 Thevenin equivalent diagram

The magnitude of load apparent power S_L is calculated as follows

$$S_L = \frac{E_{Thev}^2 Z_L}{Z_{Thev}^2 + Z_L^2 + 2Z_{Thev}Z_L \cos(\beta - \alpha)} \quad (3.4)$$

where, Z_L is the load impedance
Z_{Thev} is the Thevenin impedance
E_{Thev} is the Thevenin voltage
α is the phase angle of the load impedance
β is the phase angle of the Thevenin impedance

If considering Thevenin parameters are constant, the maximum load apparent power S_{Lmax} is then determined by differentiating $\partial S_L / \partial Z_L = 0$, which happens when $Z_L = Z_{Thev}$. Maximum load apparent power becomes:

$$S_{L\max} = \frac{E_{Thev}^2}{2Z_{Thev}[1 + 2\cos(\beta - \alpha)]} \quad (3.5)$$

Power transfer stability index is then defined by the ratio S_L/S_{Lmax}, which yields

$$PTSI = \frac{2S_L Z_{Thev}[1+\cos(\beta-\alpha)]}{E_{Thev}^2} \quad (3.6)$$

Using equation (3.6), the PTSI is calculated at every bus by using information of the load apparent power, Thevenin voltage and impedance, load impedance angle, and the Thevenin impedance angle. The value of PTSI will fall between 0 and 1. When PTSI value reaches 1, it indicates that a voltage collapse has occurred.

Thevenin voltage and impedance of a system viewed from a load bus can be determined from two different states of the system, e.g. through two load levels of the load bus while keep the system topology and generation constant. In essence, Thevenin parameters can be tracked online based on phasor measurement unit (PMU) by recursive less means square algorithm [19, 20]

4 Formulation of Voltage Stability Indices

In this section, a reduced local network is introduced. Siemens voltage criteria are formulated based on the reduced local network. A new voltage stability index called Approximate Collapse Power index (ACPI) based on quadratic approximation of PV-curve, is derived. The index, and the indices reviewed in chapter 2 are implemented in the local network. This section also sets up calculations of these indices in PSS®NETOMAC

4.1 Reduced local network

Figure 4.1 (a) shows a local network for any node j in a transmission system. The network has two portions. The first includes loads, generators, and compensation components and is presented as a load (or generator). The second includes all the lines, which are presented by the pi- equivalent circuit.

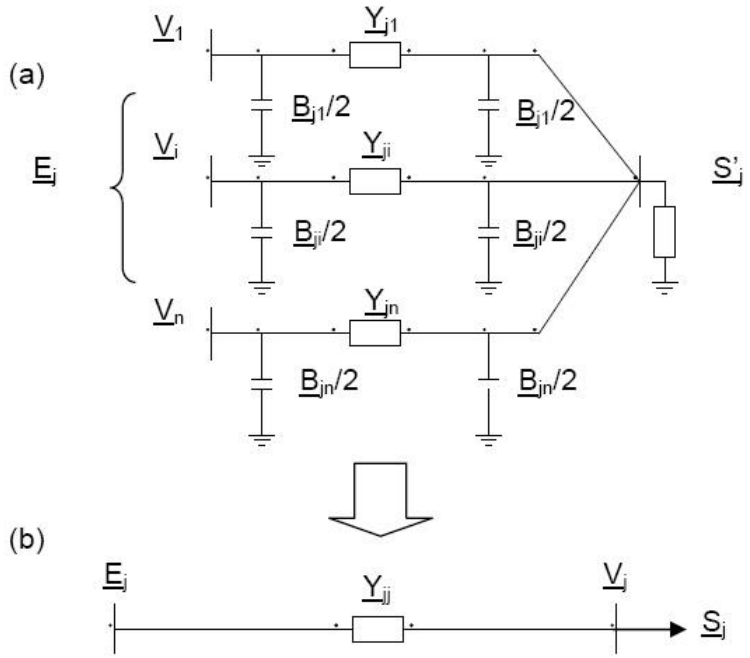

Figure 4.1 Network viewed from node j (a) reduced local network (b)

Sj, in figure 4.1 (b), is Sj' plus the reactive charging powers at one end of all transmission lines. For the local network, power flow equation written at node j gives:

$$\underline{V}_j \cdot [Y]_j[V] = \underline{S}_j^* \quad (4.1)$$

where, $[Y]_j$, row j-th admittance matrix, $[Y]_j = [-\underline{Y}_{j1} - \underline{Y}_{j2} \; +\underline{Y}_{jj} \; .. \; -\underline{Y}_{jn}]$

$\underline{Y}_{ji}$ is admittance between node j and node i:

$$\underline{Y}_{ji} = G_{ji} + i.B_{ji} = Y_{ji}.e^{i.\delta_{ji}} \text{ , i=1.. n, i}\neq\text{j..}$$

$\underline{Y}_{jj}$ is self admittance at node j:

$$\underline{Y}_{jj} = \sum_{i=1, i\neq j}^{n} \underline{Y}_{ji} = Y_{jj}.e^{i.\delta_{jj}}$$

[V], nodal voltages, $[V] = \begin{bmatrix} \underline{V}_1 \\ \underline{V}_2 \\ .. \\ \underline{V}_n \end{bmatrix}$

Expanding eq. (4.1), and letting $\frac{\sum_{i=1, i\neq j}^{n} \underline{Y}_{ji}.\underline{V}_i}{\underline{Y}_{jj}} = \underline{E}_j$ gives:

$$\underline{V}_j^*.(\underline{E}_j - \underline{V}_j).\underline{Y}_{jj} = \underline{S}_j^* \tag{4.2}$$

Equation (4.2) is the load flow equation of 2 node system shown in figure 4.1 (b). The local network is reduced to an equivalent two node system, where $\underline{E}_j$, and $\underline{Y}_{jj}$ are the equivalent voltage, and the equivalent admittance (self admittance) of the network seen from node j respectively.

Let $e_j = \frac{V_j}{E_j}$, and divide both sides of equation (4.2) over $E_j^2 Y_{jj}$ gives:

$$e_j^2 - e_j.e^{i.\psi_j} = \underline{S}_{jj},\ \psi_j = \phi_j - \theta_j \tag{4.3}$$

where, $\underline{S}_{jj} = \underline{P}_{jj} + i.\underline{Q}_{jj}$, normalized nodal power

$$\begin{bmatrix} P_{jj} \\ Q_{jj} \end{bmatrix} = \frac{1}{Y_{jj}.E_j}.\begin{bmatrix} \cos\delta_{jj} & -\sin\delta_{jj} \\ -\sin\delta_{jj} & -\cos\delta_{jj} \end{bmatrix}.\begin{bmatrix} P_j \\ Q_j \end{bmatrix} \tag{4.4}$$

Separating (4.3) into real and imagine components:

$$e_j^2 - e_j.\cos\psi_j = P_{jj} \tag{4.5}$$

$$-e_j.\sin\psi_j = Q_{jj} \tag{4.6}$$

4.2 Formulation of voltage stability indices

4.2.1 Siemens specific formulation of stability criteria

Eliminate ψ_j from equations (4.5), and (4.6) one gets a quadratic equation of e_j^2

$$\left(e_j^2\right)^2 - \left(1 + 2.P_{jj}\right).(e_j^2) + P_{jj}^2 + Q_{jj}^2 = 0 \tag{4.7}$$

The condition for existing at least one solution different to 0 of equation (4.7) are:

$$\Delta_{jj} \leq 1 \tag{4.8}$$

$$1 + 2.P_{jj} > 0 \tag{4.9}$$

where, $\Delta_{jj} = \frac{4.\left(P_{jj}^2 + Q_{jj}^2\right)}{\left(1 + 2.P_{jj}\right)^2} = \frac{4.S_{jj}^2}{(1 + 2.P_{jj})^2}$ (4.10)

Under these conditions, e_j can be expressed as:

$$e_j = \sqrt{\frac{1+2.P_{jj}}{2}.\left(1 \pm \sqrt{1-\Delta_{jj}}\right)} \quad (4.11)$$

Divide equation (1.6) over $-e_j$ and take absolute value gives:

$$\left|\sin\psi_j\right| = \left|-Q_{jj}\right| / e_j \quad (4.12)$$

At the voltage collapse point, we have $\Delta_{jj} = 1$, insert the value into equation (4.11) gives:

$$e_j = \sqrt{\frac{1+2.P_{jj}}{2}}. \quad (4.13)$$

From equations (1.13) and (1.10) with $\Delta_{jj} = 1$ gives:

$$S_{jj} = e_j^2 \quad (4.14)$$

Magnitude of $\underline{S}_{jj}$ is calculated from equation (4.4)

$$S_{jj} = \frac{S_j}{Y_{jj}.E_j^2} \quad (4.15)$$

From (1.14), (1.15), with reminding that $e_j = \frac{V_j}{E_j}$ then:

$$Y_{jj} = \frac{S_j}{V_j^2} = Y_{jL} \quad (4.16)$$

Thus, at the voltage collapse point load admittance is equal to the self admittance of the network. The condition is corresponding with the condition for maximum power transfer from the network to load at node j.

Wang [21] proposed two indices related to voltage collapses which are defined according to (4.10) and (4.12), where Δ_{jj} calls Local Load Index (LLI), and $|Q_{jj}/e_j|$ Phase Angle Index (PAI). In normal operation, the value of the indices varies between 0 and 1. If the indices are closed to zero, the voltage at bus j is considered stable, and if one index is unity, a voltage collapse is said to occur.

Using equations (4.10) and (4.12), the indices are calculated at every nodes of the network using information of the load power, the node voltages, and equivalent admittance of the network seen from the node. The system is collapsed if the indices of any node reach 1.

4.2.2 Approximate collapse power index

In [22], the critical active power of a system at a load bus is estimated by quadratic approach approximation of PV-curve. In a system, if a PV curves of node i assumed to be built by solving the load flow equations:

$$P_i = P_{i0}(1+d\lambda) = \sum_{j=1}^{N} V_i V_j Y_{ij} \cos(\delta_i - \delta_j - \theta_{ij}) \quad (4.17)$$

$$Q_i = Q_{i0}(1+q\lambda) = \sum_{j=1}^{N} V_i V_j Y_{ij} \sin(\delta_i - \delta_j - \theta_{ij}) \quad (4.18)$$

where, P_{i0}, Q_{i0} are load active, reactive power at the base case

λ is the loading factor

d, q are relative load ding factors of active, reactive load power increase respectively

V_i (V_j) is voltage magnitude at node i (node j)

Y_{ij} is the admittance of the line connecting node i and node j

δ_i (δ_j) is phase angle of voltage phasor at node i (node j)

θ_{ij} is phase angle of the admittance of the line connecting node i and node j

The quadratic approach assumes a second-order approximation for the plot of $V_i = f(\lambda)$ defined as:

$$\lambda_i = a_i V_i^2 + b_i V_i + c_i \tag{4.19}$$

The first-order derivative $dV_i / d\lambda_i$ and the second-order derivative $d^2V_i / d\lambda_i^2$ are found as follows:

$$\frac{d\lambda}{dV_i} = 2a_i + b_i \tag{4.20}$$

$$\frac{dV_i}{d\lambda} = \frac{1}{2a_i + b_i} \tag{4.21}$$

$$\frac{d^2V_i}{d\lambda^2} = -2a_i\left(\frac{dV_i}{d\lambda}\right)^3 \tag{4.22}$$

Coefficients a_i, b_i, and c_i are found by solving the equations as follows:

$$a_i = -\frac{d^2V_i / d\lambda^2}{2(dV_i / d\lambda)^3} \tag{4.23}$$

$$b_i = \frac{1}{dV_i / d\lambda} - 2a_iV_i \tag{4.24}$$

$$c_i = \lambda - a_iV_i^2 - b_iV_i \tag{4.25}$$

where, V_i is the voltage calculated from the load flow equations, and the first and second order derivatives $dV_i / d\lambda_i$ and $d^2V_i / d\lambda_i^2$ are calculated from the appendix 1

The critical voltage which corresponding to the maximum coefficient $\lambda_{c,i}$ is obtained by taking (4.20) equal to zero, which gives:

$$V_{c,i} = -b_i / (2a_i) \tag{4.26}$$

The maximum coefficient $\lambda_{c,i}$ is obtained by inserting $V_{c,i}$ into (4.19):

$$\lambda_{c,i} = a_iV_{c,i}^2 + b_iV_{c,i} + c_i \tag{4.27}$$

Based on the approximation of the collapse active power, a new index, Approximate Collapse Power Index (ACPI), is defined as:

$$ACPI = \frac{P_i}{P_{c,i}} = \frac{1}{1 + d\lambda_{c,i}} \tag{4.28}$$

ACPI will vary from the range from 0 to 1. At low load levels, the index is close to 0. When the system goes to critical point, ACPI reaches unity.

4.2.3 Applying of previous indices in the reduced local network

It shows that from a load bus, the system can be viewed as an equivalent voltage $\underline{E}j$ connecting with the load bus through a self admittance $\underline{Y}_{jj}$. It is suitable to apply previous indices based on the reduced local network defined in figure 4.1

- Line stability index: applying the same criteria to the reduced local network, formula (3.1) becomes:

$$Lmn = \frac{-4Q\sin\theta}{Y_{jj}([E_j\sin(\delta + \theta)]^2} \tag{4.29}$$

where, Q is load reactive power

θ is the self admittance phase angle

δ is the angle difference between the equivalent voltage $\underline{E}_j$ and the load voltage $\underline{V}_j$

Y_{jj} is the self admittance magnitude of the local network viewed from the load bus

E_j is the equivalent voltage magnitude of the local network viewed from the load bus

- Voltage collapse proximity index: using the equivalent parameters of the reduced local network, index VCPI from (3.2) is rewritten as:

$$VCPI_j = \left| 1 - \frac{\underline{E}_j}{\underline{V}_j} \right| \tag{4.30}$$

where, $\underline{E}_j$ is the equivalent voltage phasor of the local network viewed from the load bus

$\underline{V}_j$ is the load bus voltage phasor.

- Line power transfer stability index: to implement the index in the reduced local network, there are two assumptions. Beside power factor of the load is assumed constant, the equivalent voltage magnitude E_j is assumed not vary with the load voltage. Under these assumptions, PTSI can be rewritten as follows:

$$PTSI = \frac{2S_L[1+\cos(\beta-\alpha)]}{Y_{jj}E_j^2} \tag{4.31}$$

where, S_L is the load apparent power

α is the phase angle of the load admittance

β is the phase angle of the self admittance viewed from the load bus

Y_{jj} is the self admittance of the local network viewed from the load bus

E_j is the equivalent voltage magnitude of the local network viewed from the load bus.

4.2.4 Calculating the indices in PSS®NETOMAC

All the indices are calculated based on the reduced local network. The calculations of the indices only base on the information of the load bus voltage and power, its surrounding bus voltage and the admittance between the load bus and participating buses. The indices can be easy implemented in PSS®NETOMAC based on several macros, some of which are presented in appendix A3. The calculation algorithm of the indices is shown in figure 4.2, where:

- Yij.mac: this macro reads the voltage of two ends of a branch and current flow on the branch. The output of this macro is the admittance of the branch.
- Yjj.mac: this macro evaluates the line admittance of participating line to calculate the self admittance of the local network viewed from the load bus.
- Ej.mac: this macro evaluates the line admittance of participating line, self admittance at the load bus and information of participating bus voltages. The output of this macro is the equivalent voltage of the local network viewed from the load bus.
- Finally, each index can be calculated separately using the equivalent local network parameters.

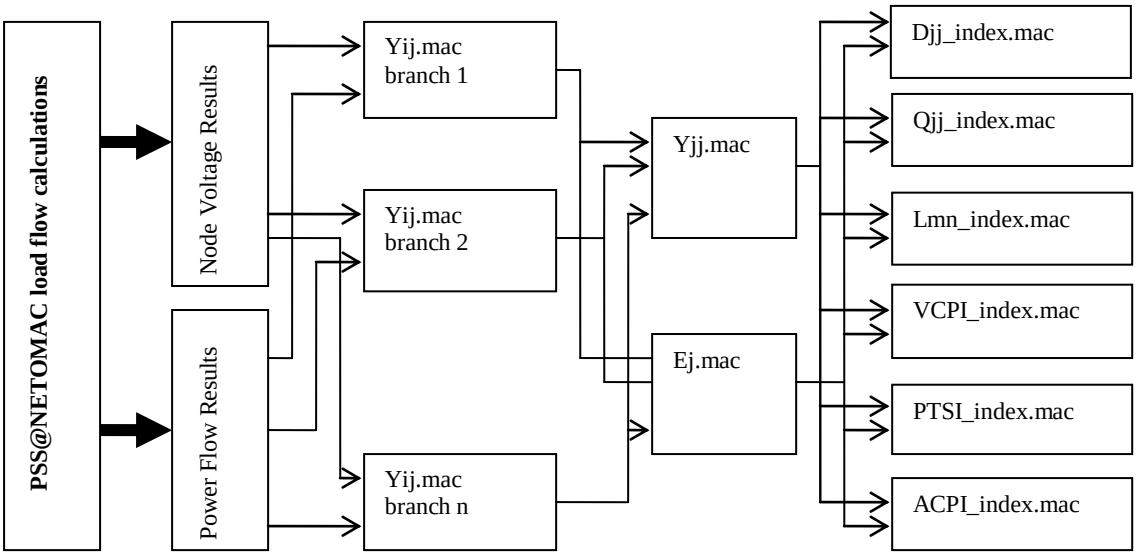

Figure 4.2 Calculation block diagram of the indices in PSS®NETOMAC

5 Simulation Results and Discussions

This section tests voltage stability indices through two test systems: 9 bus-3 generator test network and a larger test network including 414 buses, and 119 generators. In the smaller network, static analysis and dynamic simulation are implemented. In the static analysis, PV curve of the system is built by gradually increasing loads at a bus until the load flow program is diverged. Two cases are implemented, with and without considering reactive power limit of generators, to investigate the affects of reactive power limits of generators in the load flow feasibility. For dynamic simulations, the affects of AVR and OXL are examined. Line contingencies of the system are studied to show that the indices are useful for line contingency ranking. For every test, the indices are investigated and compared regarding to sensitivities. It shows that all indices have coherent performances relating to voltage stability. They are close 0 when the system is stable, and increase towards 1 when the system is more critical. Two most sensitive indices, APCI and PTSI, are used to study the larger test system for different disturbances, load increasing and line disconnections. The calculation times of indices are compared based on dynamic simulations of the larger test network.

5.1 9 bus system test

5.1.1 Description of the 9 bus test system

The system used to test the performance of the voltage stability indices includes 9 buses, 3 generators as shown in figure 5.1. The generators are equipped with auto voltage regulators and over excitation limiters (AVR, and OXL). The loads are modeled as constant power. Detailed parameters of the system are in Appendix A1.

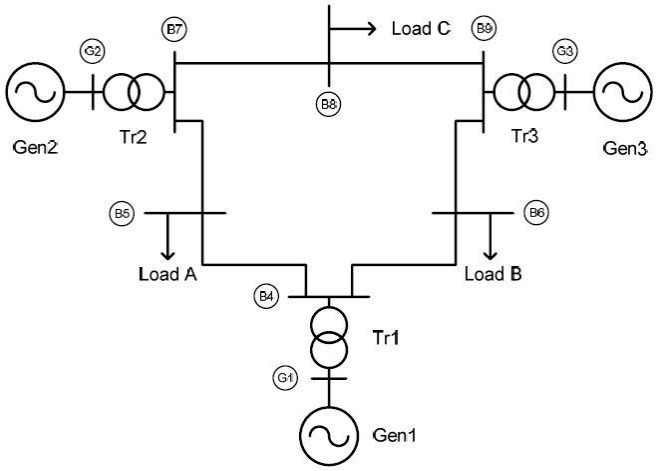

Figure 5.1 9 bus- 3 generator- test network

In the system, G1 is set as a slack bus which has constant voltage magnitude and phase while its power generation is indefinite. Setting parameters of the system for basic load level are shown in table 5.1

Bus	Type	V (p.u)	Phase (deg.)	P (MW)	Q (MVar)
G1	Slack	1.00	0	x	x
G2	PV	1.00	x	163.2	x
G3	PV	1.00	x	108.8	x
B5	PQ	x	x	-100	-50
B6	PQ	x	x	-100	-50
B8	PQ	x	x	-100	-50

Table 5.1 9 bus test network setting at base load level

In table 5.1, positive powers imply the power injecting into the system (for generators), while negative powers indicates the power consumed by the loads. All unknowns are marked as 'x' is found after load flow calculations.

5.1.2 Static analysis

In static approach, PV curves are built at every load bus by increasing load at bus 5 while the loads at bus 6, 8 are kept constant. For each load level of load at bus 5, running power flow program to get the corresponding voltages of the buses. All indices are also calculated. The increase of load is continued until the load flow is diverged. There are two cases setting for the test. In the first case, reactive power limits of generators are ignored while in the second including the reactive power limit of generators.

In this test, the maximum reactive power that load at bus 5 can consume in the first case is much higher than that in the latter. This implies that reactive power of generators is a main contributor to the loadability of the system. The loadability of the system is much smaller when considering the limit of reactive power sources.

The results show that performances of indices are in agreement to each other and to the voltage instability. At the base case, the indices are small, close 0, means that the system is stable. When the loads are higher, the indices are higher. At load level where the power flow calculation diverges, the indices close 1 indicates that the system is collapsed. Among all indices, index ACPI seem to be the most sensitive one.

With static approach, the indices are good indicators for ranking the critical bus. Since load at bus 5 is increased, the indices at the bus are increased and have highest values compared to those at bus 6, 8; this load bus is the most critical one.

5.1.2.1 Case 1 without limitation of reactive power generators

In this case, maximum of reactive power of generators are not defined. It implies that the generators are able to generate as much reactive power as the system required. During load flow calculation, voltage magnitudes of generator terminals are always constant. Table 5.2-5.4 shows the voltage of buses and corresponding indices to increasing active power load at bus 5.

P5(MW)	V5 (p.u.)	D55	|Q55/e5|	VCPI5	PTSI5	Lmn5	ACPI5
99,99	0,954	0,005	0,030	0,036	0,107	0,063	0,198
199,99	0,921	0,024	0,063	0,078	0,220	0,131	0,355
299,97	0,897	0,064	0,101	0,129	0,342	0,207	0,491
399,94	0,823	0,142	0,148	0,196	0,481	0,297	0,619
499,88	0,736	0,313	0,217	0,306	0,661	0,425	0,759

549,81	0,648	0,534	0,286	0,434	0,806	0,546	0,864
559,72	0,559	0,666	0,324	0,517	0,872	0,612	0,908

Table 5.2 Static analysis at bus 5 without considering reactive power limits of generators

P5(MW)	V6 (p.u.)	D66	|Q55/e5|	VCPI6	PTSI6	Lmn6	ACPI6
99,99	0,955	0,006	0,031	0,038	0,112	0,066	0,205
199,99	0,946	0,006	0,032	0,039	0,114	0,067	0,208
299,97	0,932	0,006	0,033	0,040	0,117	0,069	0,213
399,94	0,912	0,007	0,034	0,042	0,122	0,072	0,221
499,88	0,878	0,008	0,037	0,045	0,131	0,078	0,235
549,81	0,842	0,009	0,040	0,049	0,142	0,084	0,251
559,72	0,821	0,010	0,042	0,051	0,149	0,088	0,261

Table 5.3 Static analysis at bus 6 without considering reactive power limits of generators

P5(MW)	V8(p.u.)	D88	|Q88/e8|	VCPI8	PTSI8	Lmn8	ACPI8
99,99	0,962	0,003	0,022	0,027	0,080	0,047	0,152
199,99	0,953	0,003	0,023	0,027	0,081	0,048	0,155
299,97	0,940	0,003	0,023	0,028	0,083	0,049	0,158
399,94	0,923	0,003	0,024	0,029	0,086	0,051	0,163
499,88	0,896	0,004	0,026	0,031	0,091	0,054	0,172
549,81	0,868	0,004	0,027	0,033	0,097	0,057	0,181
559,72	0,852	0,005	0,028	0,034	0,101	0,059	0,187

Table 5.4 Static analysis at bus 8 without considering reactive power limits of generators

From table 5.2-5.4, it shows that when the load level at bus 5 increased the voltage at that bus decrease while the indices increase. At the load level P5= 559.72 MW, the indices are close 1. It shows that the system is near a collapse point. If the load at bus 5 is increased beyond this level, the power flow calculation diverges.

The index variations to load levels at bus 5 are plotted in figure 5.2

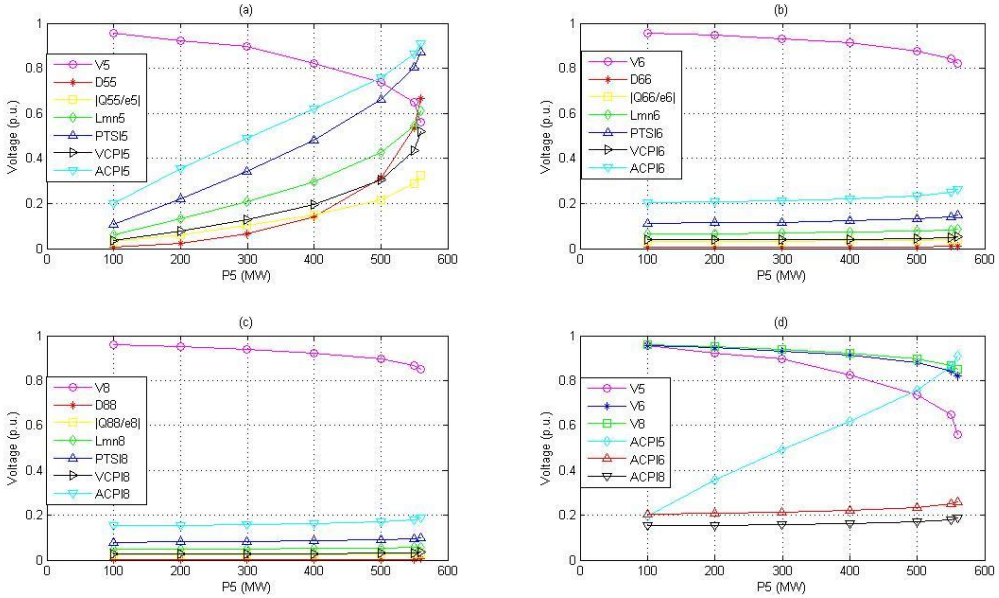

Figure 5.2 Static analysis at bus 5 without reactive power limits of generators

Figure 5.2 (a), (b), and (c) are the variations to load levels at bus 5 of voltage and indices at bus 5, 6, and 8 respectively. At every bus, it shows that when the load level grows the voltage at that bus decreases while the indices increase. The variation of voltage and indices at bus 5 grow sharply since the system is stressed directly from this bus while at bus 6 and bus 8 the changes are slowly. At the point close to the maximum power point, the indices at bus 5 are close unity. The figure shows that index ACPI is the most sensitive and linear one because it has higher value and goes faster than other indices when the load at bus 5 increases.

From figure 5.2 (a), it can be seen that index D55 are the smallest at lower load level at bus 5 (e.g. P5=100-400 MW). However, it increases sharply, greater than |Q55/e5|, VCPI5, and Lmn5 when the load level is higher.

From figure 5.2 (b), and (c), it shows that the voltages change slowly, and the indices are almost unchanged when the load level at bus 5 grows. The reason is that the loads at these buses are constant so the changes of indices depend almost on the drop of voltage at these bus and their surrounding buses.

Figure 5.2 (d) shows more clearly the relation of voltage and indices with load levels at bus 5. It presents the voltages and index ACPI at each bus. From the figure, at the base case, the voltages at every bus are at high level, and the value of VCPI6 is highest, which implies that bus 6 is the most critical one. At higher load level at bus 5, the voltages are smaller, and index VCPI5 is the highest. It shows that bus 5 is the most critical bus in the system.

5.1.2.2 Case 2 including reactive power generator limitations

In load flow model, it is necessary to consider the ability of generators whether it is available to supply reactive power demands of the system. To determine the range of reactive power limits of generators, capability curve of the generators can be used [13]. The capability curve of generator varies with the excitation voltages. This causes impossible to calculate exactly the range of reactive power of generators. However, in this study, the value can be estimated by assuming the excitation voltage is 1 (p.u.). Notice that the initial value of generator G2, and G3 are at its rating power, therefore the maximum reactive power of these generators are determined directly through the rating power, and the power factor of the generators. The maximum reactive power of G2, and G3 are shown in table 5.5

	G2	G3
Rating (MVA)	192	128
Power factor	0.85	0.85
Active power (MW)	163,2	108,8
Maximum reactive power (MVar)	101,6	64,7

Table 5.5 Maximum reactive power of generators

With the setting of reactive power limit of generators above, power flow calculations are performed the same as in previous case by increasing load at bus 5. The results of this test are shown in table 5.6-5.8, and in figure 5.3

P(MW)	V5 (p.u.)	D55	|Q88/e8|	VCPI5	PTSI5	Lmn5	ACPI5
99,99	0,954	0,005	0,030	0,036	0,107	0,063	0,198
199,99	0,920	0,024	0,063	0,078	0,221	0,131	0,356
299,97	0,817	0,085	0,116	0,149	0,387	0,235	0,535
350,04	0,718	0,183	0,167	0,225	0,534	0,333	0,662
359,98	0,681	0,233	0,188	0,257	0,588	0,372	0,705
365,10	0,647	0,284	0,207	0289	0637	0,407	0,741

Table 5.6 Static analysis at bus 5 considering reactive power limits of generators

P(MW)	V6 (p.u.)	D66	|Q88/e8|	VCPI6	PTSI6	Lmn6	ACPI6
99,99	0,955	0,006	0,031	0,038	0,112	0,066	0,205
199,99	0,943	0,006	0,032	0,039	0,114	0,068	0,209
299,97	0,876	0,008	0,037	0,045	0,132	0,078	0,235
350,04	0,809	0,011	0,043	0,053	0,153	0,091	0,267
359,98	0,783	0,013	0,046	0,056	0,162	0,096	0,280
365,10	0,759	0,014	0,049	0,060	0,172	0,102	0,294

Table 5.7 Static analysis at bus 6 considering reactive power limits of generators

P(MW)	V8 (p.u.)	D88	|Q88/e8|	VCPI8	PTSI8	Lmn8	ACPI8
99,99	0,962	0,003	0,022	0,027	0,080	0,047	0,152
199,99	0,950	0,003	0,023	0,027	0,082	0,048	0,155
299,97	0,863	0,004	0,028	0,033	0,098	0,058	0,183
350,04	0,777	0,007	0,034	0,041	0,120	0,071	0,218
359,98	0,744	0,008	0,037	0,045	0,131	0,077	0,233
365,10	0,714	0,009	0,040	0,049	0,141	0,084	0,249

Table 5.8 Static analysis at bus 8 considering reactive power limits of generators

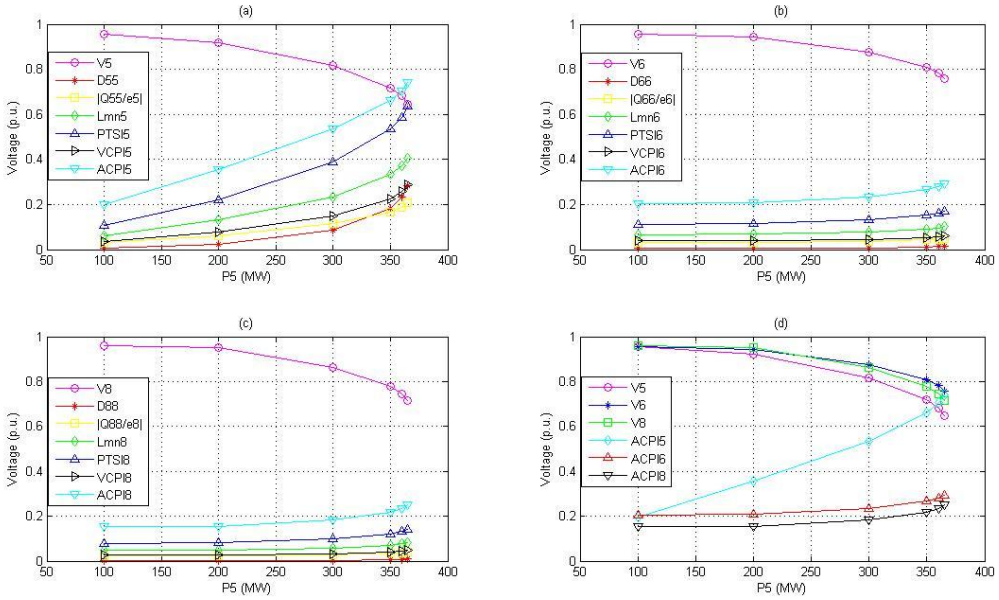

Figure 5.3 Static analysis considering reactive power limits of generators

Figure 5.3 (a), (b), and (c) are the relations of voltage and indices corresponding to load level at bus 5 for bus 5, 6, and 8 respectively. The performance of voltages and indices at each node are the same as in previous case. When the load level at bus 5 is higher, the voltages at every bus are lower and the indices are higher. However, the difference is that the maximum loading power at load 5 is only 365.10 MW, much smaller than that in the previous case. The difference of voltages, and index performances to load level at bus 5 at two cases is recognized more clearly in figure 5.4.

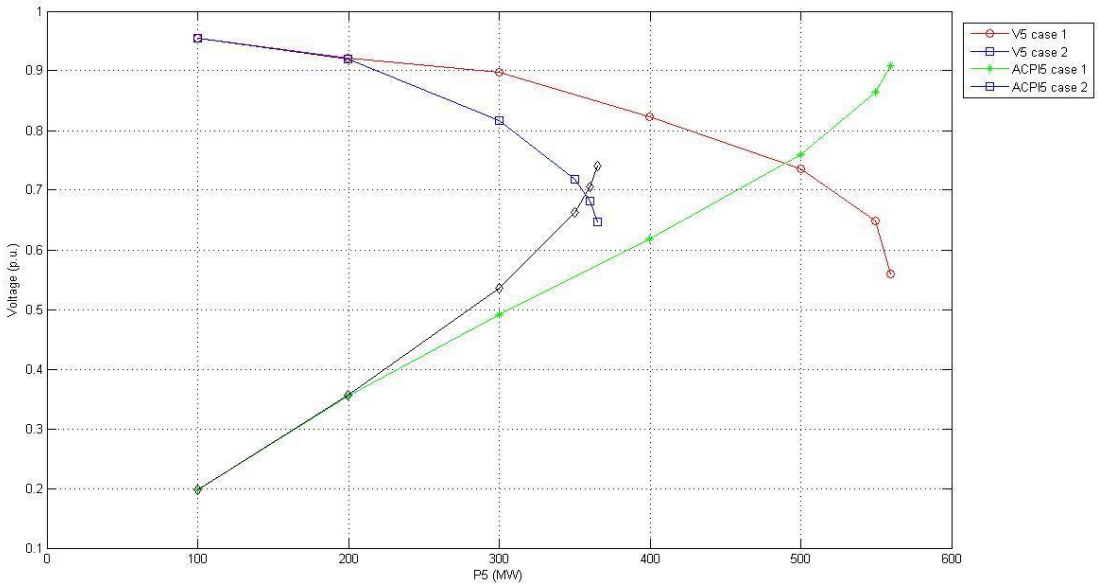

Figure 5.4 Static analysis of bus 5 at two cases

Figure 5.4 shows the relations between voltage V5 and index ACPI5 in two cases. From this figure, it shows that when the system is at low load level, the voltage and the index in two cases are equal. When the load is higher, the voltage and index change steeper for the case considering reactive power limit. This is due to the reason that the generators have supplied all its reactive power. From modeling as PV nodes which have constant terminal voltages, generators are changed into PQ node, its voltage is decreased when the load increases. This shows that considering reactive power limit of generators will reduce the ability of the system regarding to voltage stability.

5.1.2.3 Remarks of static tests

Thorough the static analysis, some remarks are pointed out as following:

- All indices are in agreement with each other and coherent with voltage stability of the system
- The indices at each bus are sensitive with the change of load at that bus only, e.g. ACPI5 changes sharply when load at bus 5 increases while ACPI6, and ACPI 8 are almost unchanged. Therefore, the indices are useful to evaluate the critical bus in a power system.
- Index Djj is not sensitive at low load level but it gets higher sensitivity than |Qjj/ej|, VCPIj, Lmnj, when the load is close to critical point.
- ACPI and PTSI seem to be the most sensitive indices to the load change.

5.1.3 Dynamic analysis

In the dynamic simulation of voltage collapse for the 9 bus test system, two operating conditions have been considered to investigate the effect of the AVR and OXL. The contingency considered for the operating conditions is by increasing the static load at bus 5 at a rate of 0.05 (p.u./sec). The power at bus 5 is defined as follows:

$$P_t = P_0(1+0.05*t) \text{ (MW)} \quad (5.1)$$

$$Q_t = Q_0(1+0.05*t) \text{ (MVar)} \quad (5.2)$$

During simulation, the indices are calculated and their performances are then compared. The system is said collapse if any of the indices reaches unity.

5.1.3.1 Effects of AVR and OXL

Case1: The first operating condition considers only static loads connected at buses 5, 6 and 8. The voltage collapse indicators, Djj, PTSI, VCPI, Lmn, and VCPI at the load buses 5, 6 and 8 are plotted against time as shown in Figure 5.5

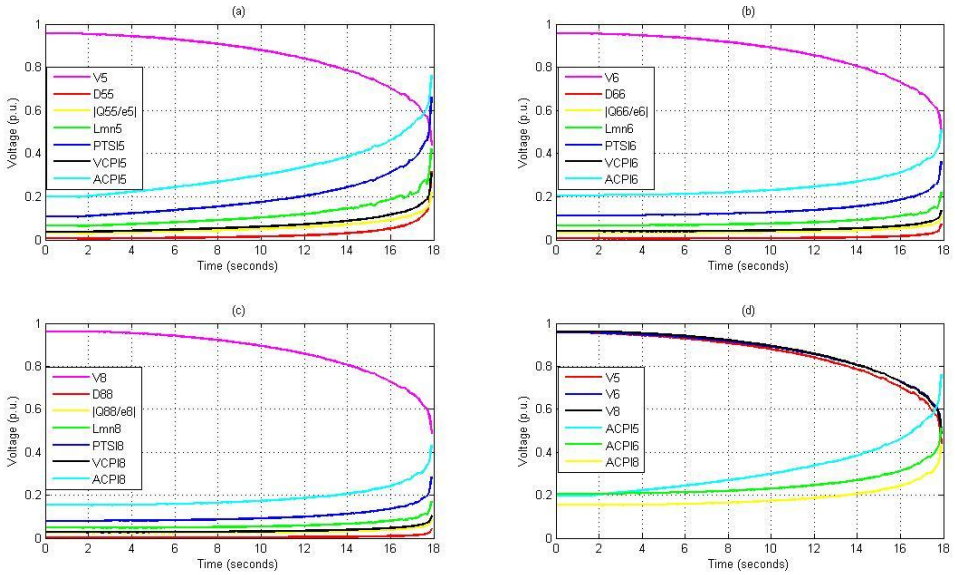

Figure 5.5 Dynamic simulations without considering AVR and OXL

From the figure, it can be seen that the indices increase with time as loads are increased and the indicators at bus 5 give the highest values compared to the indicators at bus 6 and 8. The figure also shows that system voltage collapse occurs at time t = 18 sec

Case2: The second operating point incorporates both AVR and OXL in the generators. The result is shown in figure 5.6.

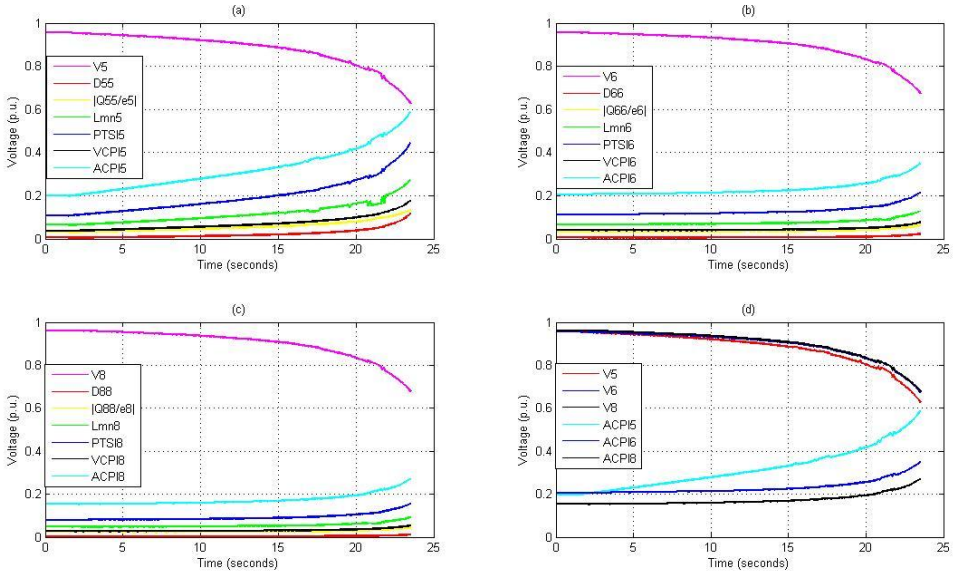

Figure 5.6 Dynamic simulations with affects of AVR and OXL

For this case, voltage collapse occurs at 23.5 sec which shows that voltage collapse occurs later than for the case without AVR and OXL. This is because of the effect of the AVR and OXL which maintain a constant generator voltage by increasing the field current while load is increased.

5.1.3.2 Line contingencies

This section tests the performance of indices according to line contingencies using dynamic simulations. The system is equipped with AVR and OXL. After each line contingency, the system variables change, the indices are recorded at the time when the system goes to steady state. The results of the test are shown in tables 5.9-5.11 and figure 5.7.

Line Disconnection	V5 (p.u.)	D55	|Q55/e5|	VCPI5	PTSI5	Lmn5	ACPI5
No	0.954	0,005	0,030	0,036	0,107	0,063	0,198
LB7-B8	0,953	0,005	0,030	0,037	0,108	0,063	0,199
LB8-B9	0,946	0,005	0,031	0,037	0,109	0,064	0,201
LB9-B6	0,937	0,006	0,031	0,038	0,111	0,066	0,204
LB6-B4	0,957	0,005	0,030	0,036	0,107	0,063	0,197
LB4-B5	0,912	0,027	0,067	0,083	0,233	0,139	0,371
LB5-B7	0,908	0,023	0,062	0,077	0,27	0,129	0,352

Table 5.9 Contingency analysis at bus 5

Line Disconnection	V6 (p.u.)	D66	|Q66/e6|	VCPI6	PTSI6	Lmn6	ACPI6
No	0,955	0,005	0,031	0,038	0,112	0,066	0,205
LB7-B8	0,933	0,006	0,033	0,040	0,117	0,069	0,213
LB8-B9	0,962	0,006	0,031	0,037	0,110	0,065	0,202
LB9-B6	0,906	0,028	0,068	0,084	0,235	0,141	0,375
LB6-B4	0,912	0,027	0,067	0,083	0,232	0,139	0,371
LB4-B5	0,958	0,006	0,031	0,038	0,111	0,066	0,204
LB5-B7	0,933	0,006	0,033	0,040	0,117	0,069	0,213

Table 5.10 Contingency analysis at bus 6

Line Disconnection	V8 (p.u.)	D88	|Q88/e8|	VCPI8	PTSI8	Lmn8	ACPI8
No	0,962	0,003	0,022	0,027	0,080	0,047	0,152
LB7-B8	0,904	0,024	0,063	0,078	0,219	0,131	0,354
LB8-B9	0,935	0,009	0,038	0,046	0,135	0,080	0,240
LB9-B6	0,964	0,003	0,022	0,027	0,079	0,047	0,152
LB6-B4	0,950	0,003	0,023	0,027	0,082	0,048	0,156
LB4-B5	0,947	0,003	0,023	0,028	0,082	0,048	0,156
LB5-B7	0,960	0,003	0,022	0,027	0,080	0,047	0,153

Table 5.11 Contingency analysis at bus 8

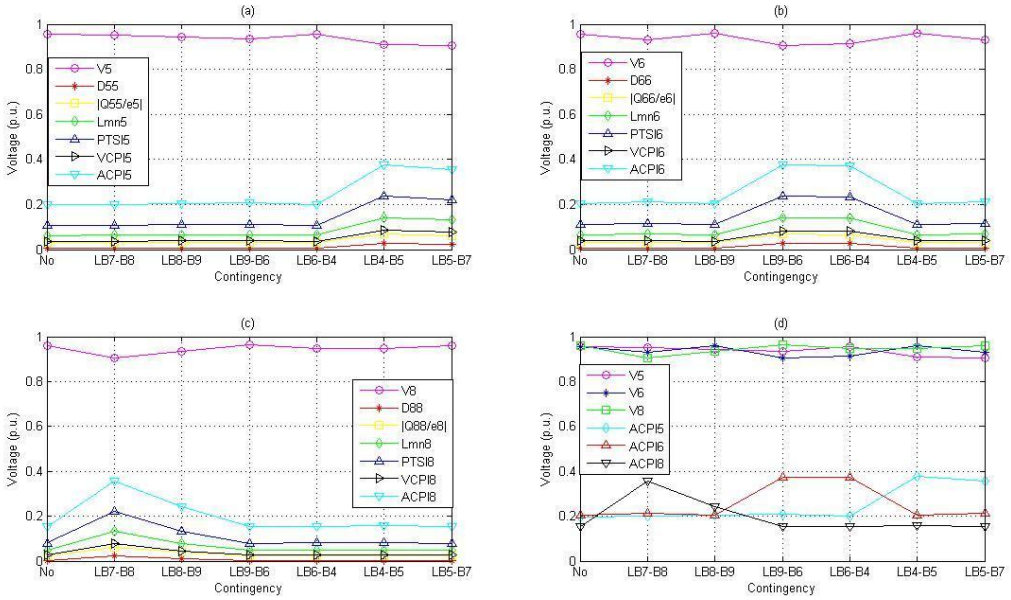

Figure 5.7 Line contingencies and index performances

In the tables 5.9-5.11, and figure 5.7, 'No' is corresponding to the normal operating condition. Figures 5.7 (a)-(c) illustrate the variations to different line contingencies of the indices at bus 5, 6, and 8 respectively. From the figures, it shows that from the normal operating condition the indices jump to higher values when a line is disconnected. The indices have significant value at bus where has direct connection with the disconnected line. For example, the indices at bus 5 are higher than those at bus 6, 8 as the disconnected lines are 'LB4-LB5', 'LB5-LB7'. Similarly, the indices at bus 6, 8 are significantly high as these are 'LB9-B6', 'LB6-B4', and 'LB7-B8', 'LB8-B9', respectively. The reason is that when a line is switch off, the self admittance of the reduced local network at node j, which directly connected to the disconnected line are decreased. This causes the loadability of the reduced local network lessen and hence the indices jump up.

The sensitivity of the indices to the line contingencies are also shown clearly in the figure. It shows that Djj has the smallest sensitivity while ACPI has the highest. Relying on the index, line contingency ranking can be obtained by set ACPIj as the maximum value of ACPI5, ACPI6, and ACPI8, then sorting the line contingencies according to ACPIj. Table 5.12 shows the rank of line contingencies based on the evaluation of the index.

Line Disconnection	Vj (p.u.)	Djj	|Qjj/ej|	VCPIj	PTSIj	Lmnj	ACPIj	Rank
LB4-B5	0,91	0,028	0,068	0,085	0,236	0,141	0,376	1
LB9-B6	0,905	0,028	0,068	0,084	0,236	0,141	0,375	2
LB6-B4	0,912	0,027	0,067	0,083	0,233	0,139	0,372	3
LB5-B7	0,906	0,024	0,063	0,078	0,221	0,131	0,356	4
LB7-B8	0,903	0,024	0,063	0,078	0,22	0,131	0,355	5
LB8-B9	0,934	0,009	0,038	0,046	0,135	0,08	0,241	6
No	0,962	0,003	0,022	0,027	0,08	0,047	0,152	7

Table 5.12 Line contingency ranking with index ACPI

In table 5.12, Vj, and Djj to Lmnj are voltage, and indices which are corresponding to ACPIj. From the table, it points that 'LB4-B5' outage is the most severe line contingency in the system.

5.1.3.3 Remarks of the dynamic tests

From the dynamic analysis, some remarks are pointed out as followings:

- Effects of AVR and OXL are to strengthen the system regarding to voltage instability by increasing excitation voltage of generators so that maintaining the voltage at generators terminals.
- Performances of the indices in dynamic simulations are coincided with them in the static analysis. The indices are small, close to 0 at lower load levels and they move towards 1 when the load increases to the loadability limit.
- PTSI and ACPI seem to be the most sensitive and linear indices compared to others. A comparison of these indices regarding to sensitivity is shown in table 5.13, where more + sign indicates better sensitive

Indices	Djj	|Qjj/ej|	VCPI	PTSI	Lmn	ACPI
Sensitivity	+	+	+	+++	++	++++

Table 5.13 Sensitivity comparison of the indices

5.2 Larger network test

Previous parts have tested the performances of indices based on the 9 bus test system. The results show that two indices ACPI and PTSI are sensitive and linear to voltage instability of the system. In this section, these indices are applied in a larger test network to evaluate the feasibility of the indices in a more practical network.

5.2.1 Description of the larger test network

The test network is built based on a practical power system including 119 Generators, 527 transmission lines, 261 transformers and 414 nodes. An overview of the network is illustrated in figure A.2 in the appendix.

The power system consists of three parts: the north, center, and the south. In normal operating condition, the total generating power is 18.67 GW out of 26.36 GW. There are 4 high voltage levels 500 kV (80 nodes and 180 transmission lines), 230 kV (80 nodes and 180 lines), 115 kV (199 nodes and 314 lines) and 69 kV (4 nodes and 2 lines). The center and southern areas are connected through long tie-lines near 800 km. High load increase in the southern areas, or line outages in the tie-lines could cause severe problem to the system. These contingencies will be investigated in the test.

The test network is modeled in PSS®NETOMAC with the features as followings:

- Synchronous machines are modeled based on Park model.
- There are 24 generators are equipped speed governor of either IEEEG1 type (Figure A.6 a) or HYGOV type (Figure A.6b). They are both IEEE standard governors and defined in PSS® NETOMAC database.
- There are three types of AVR being used by all of 119 generators. They are IEEET1 type (Figure A.5a), EXAC4 type (Figure A.5b), SCRX type (Figure A.5c).

5.2.2 Load increasing

As mention earlier, load increasing in the south could make a severe problem to the network. In this case, bus SRT___00 is chosen for studying. This bus is an important bus in the southern area which

connects to the center area e.g. through the tie lines ‘L_00255’, and ‘L_00256’ and connects with a big power plant at bus KN___03 in the area through 230 kV parallel transmission lines ‘L_00239’, and ‘L_00240’.

To analyze bus SRT___00, it is necessary to know the connection of this bus with its neighbor buses, which form a local network. Figure 5.9 shows the network topology of the local network.

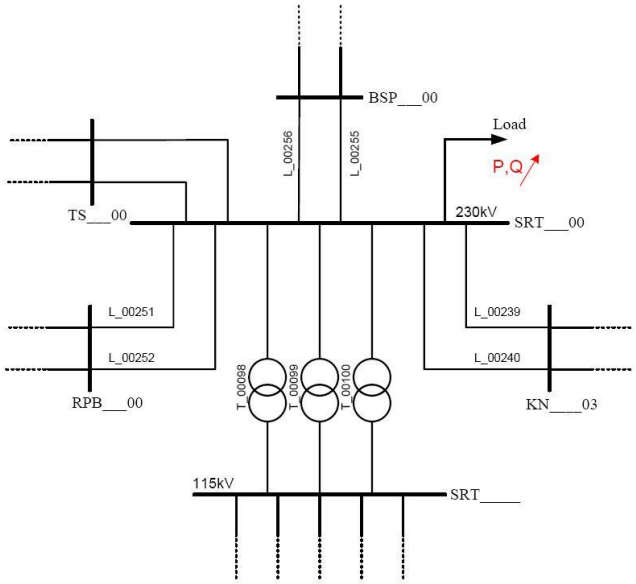

Figure 5.8 Local network of bus SRT___00

The base load at bus SRT__00 is modeled as constant power load $P_0+jQ_0=300+150j$ MVA. To simulate the contingency, from the base case the load is increasing with a rate of 0.02 p.u./ sec. The load at time t is as followings:

$$P_t = P_0(1+0.02*t) \text{ (MW)} \tag{5.6}$$

$$Q_t = Q_0(1+0.02*t) \text{ (MVar)} \tag{5.7}$$

To apply the indices at the bus in PSS®NETOMAC, several macros have been built like those for the previous 9 bus system test as shown in figure 4.2. The results of the simulation are shown in figure 5.10.

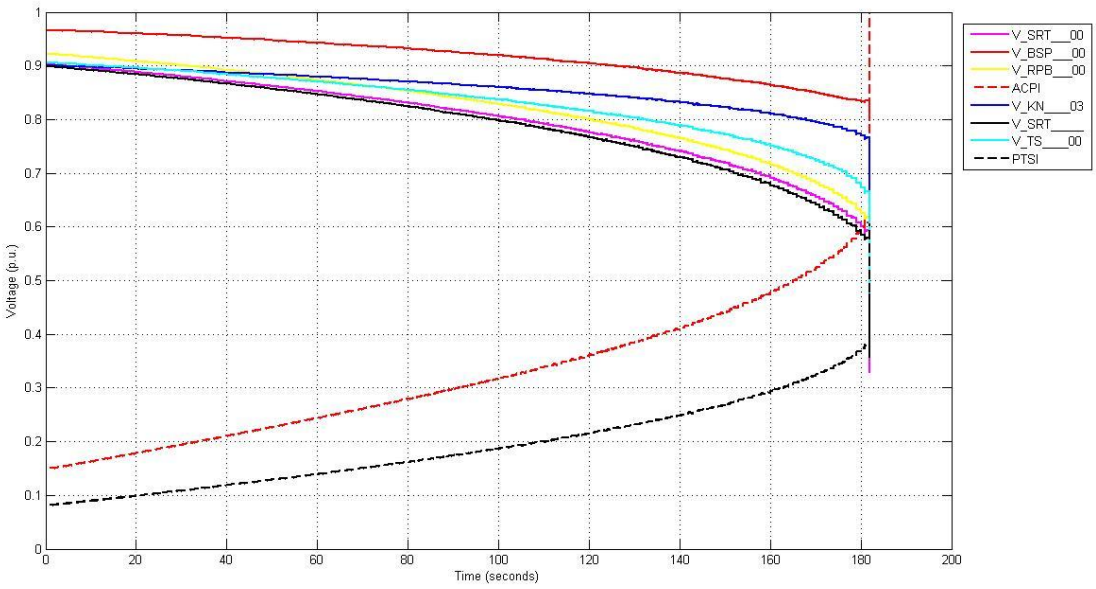

Figure 5.9 Load increasing at bus SRT_00

Figure 5.10 shows that when load at bus SRT__00 increase, the voltages at bus SRT___00 and its surrounding buses decrease while the indices PTSI, and ACPI increase. The system is collapsed at t= 180s, when the voltage at SRT__00 is 0.59 (p.u.), index ACPI at 0.60, and index PTSI at 0.39. The results show that the performances of the indices are sensitive and linear to the increasing of the load at bus SRT_00 and index ACPI has better performance compared to PTSI.

5.2.3 Disconnection of transmission lines

Bus SRT___00 connected to bus KN____03 where has a big power plant with a capacity of 710 MW. There are two transmission lines in parallel connecting these buses. If there is an outage of these transmission lines, a high voltage drop could occur at bus SRT___00. Figure 5.11 illustrates a line contingency.

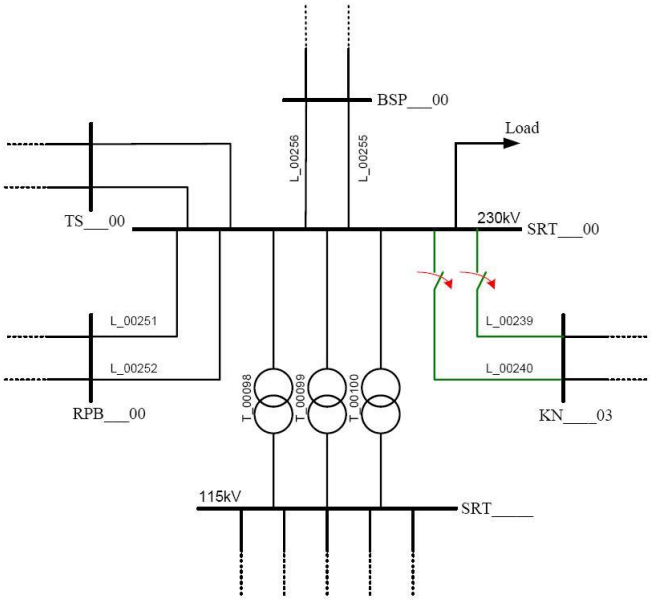

Figure 5.10 Line contingencies in the larger test network

In this test, a scenario of line outages is applied to investigate the behaviors of the indices. At 5s, a transmission line of the two parallel lines connecting these buses is switched off. Then after 15s, the next line is outage. The voltages at bus SRT___00 and its neighbor buses and indices ACPI, PTSI are calculated and illustrated in figure 5.12. Some interesting values are shown in the table 5.14

Time (s)	V_SRT___00	V_BSP___00	ACPI	PTSI
0	0.902	0.966	0.15	0.082
5	0.898	0.964	0.168	0.093
25	0.893	0.959	0.191	0.108
33	0.271	0.824	0.997	0.276

Table 5.14 Index performance according to line contingencies

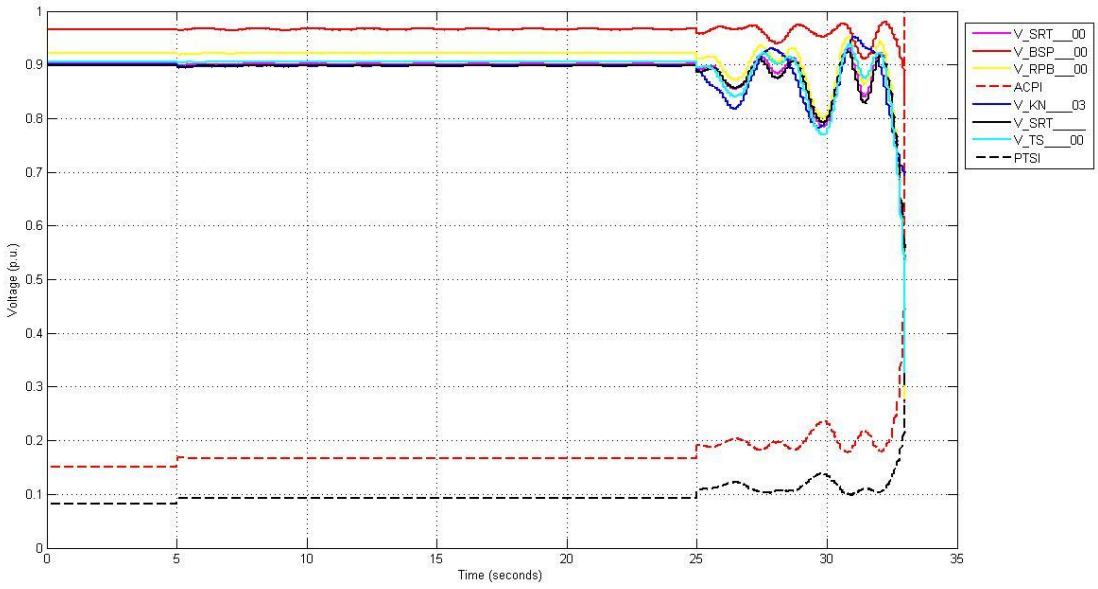

Figure 5.11 Disconnection of transmission lines in the larger test network

From figure 5.12, and data table 5.14, it shows that from 0 to 5s, the system is operating at the base case condition. The voltage at bus SRT___00 is 0.902 (p.u.), and the indices ACPI, and PTSI are approximately 0.15 and 0.082 respectively. At 5s, the transmission line 'L_00255' is switched off. The voltage at bus SRT___00 deceases to 0.898, while ACPI jumps to 0.168, and PTSI jumps to 0.093. The indices are higher means that the system becomes more critical to voltage problem. At 25s, another transmission line 'L_00252' is outage. The voltage at bus SRT___00 is down to 0.893 (p.u), while the ACPI and PTSI jump to higher values at 0.191 and 0.108, respectively. At this time, after two transmission lines connecting bus RT____00 and KN____03 are disconnected, the system become unstable, the voltages at buses and the indices fluctuate. At 33s, when the system is quite close to voltage collapse, the voltage at bus SRT___00 is 0.271 (p.u), and index ACPI is 0.997. The system becomes collapsed afterward.

5.2.4 Time of calculations

In a dynamic simulation in PSS@NETOMAC, it is able to perform variant calculations, where load flow results are calculated under different variations of data parameters, machine connection modes, operating conditions and disturbances.

The calculation time of a variant calculation (Tv) where a voltage stability index is implemented at node SRT__00 in the larger test network (e.g. index ACPI) and a line contingency is simulated in the variant calculation can be illustrated as in figure 5.13. In the figure, dt1 is the period of time to calculate load flow results, dt2 is the period of time to calculate equivalent parameters of the reduced local network, and dt3 is the period of time to calculate the index.

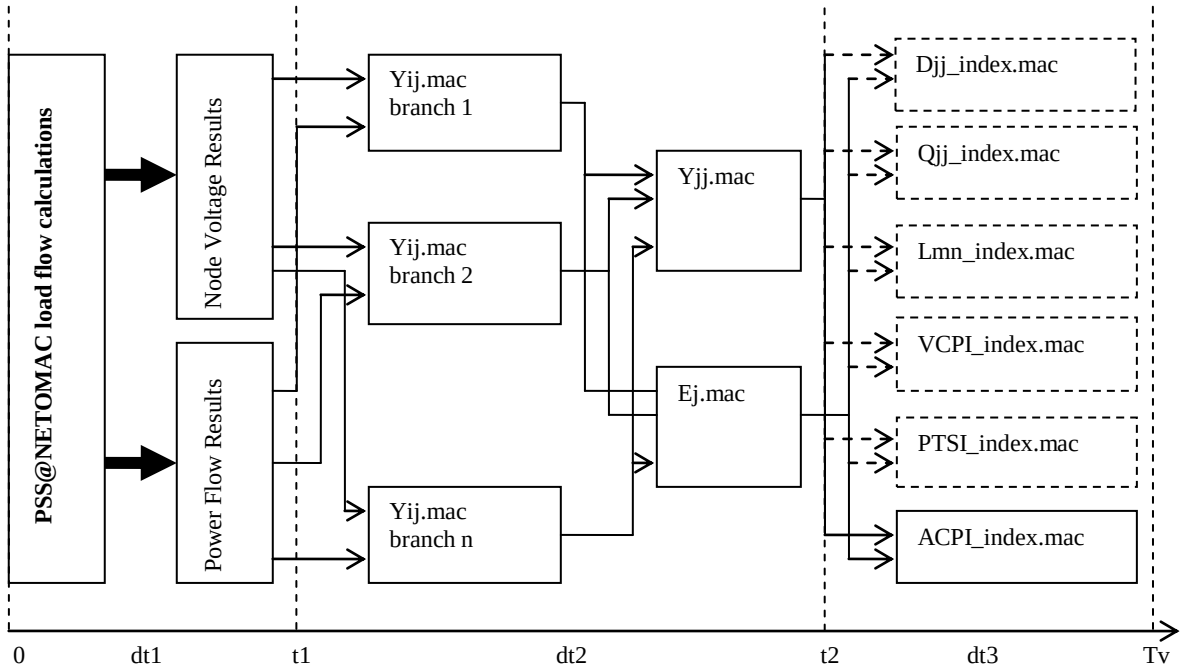

Figure 5.12 Calculation time of an index in a variant calculation

The total simulation time (Tt) is the sum of all calculation time of variant calculations. From appendix A4, it shows that Tt is proportional to number of variant calculations. Besides, it also depends on the integration time step (dt), and simulation time of each variant calculation (Tsim). The total simulation time can be expressed as follows:

$$Tt=Nc*Tv \quad (5.8)$$

where, Nc is number of variant calculations

Tv is the calculation time of a variant calculation

If a dynamic simulation is repeated in a way that in each case, a different index is implemented then the calculation time of each index (different dt3) can be compared by comparing the total simulation time (different Tt) of each case.

Figure 5.13 shows that the calculation time of a variant calculation can be separated into two parts: dt1 plus dt2, which is the same if implementing different indices, and dt3, which is different if implementing different indices. Similarly, the total simulation time can be separated into Base Calculation Time (BCT), and Individual Calculation Time (ICT), which are defined as follows:

$$BCT= Nc*(dt1+dt2) \quad (5.9)$$

$$ICT=Nc*dt3 \quad (5.10)$$

where, Nc is number of variant calculations

dt1 is the calculation time of load flow results

dt2 is the calculation time of the reduced local network parameters

dt3 is the calculation time of the index.

Then the total simulation time can be written as follows:

$$Tt=BCT+ICT \quad (5.11)$$

In this test, a dynamic simulation evaluating line contingencies in the larger test network is performed. The index ACPI is calculated at node SRT__00. The line contingencies are disconnections of lines terminating at node SRT__00, which includes 11 lines. The simulation was set up with a time step dt equal 20 ms, 11 variant calculations (each variant calculation is corresponding to one line contingency), and simulation time Tsim equal 50 ms. The total simulation time of two cases are measured to compare BCT and ICT. In the first case, the macro calculating index ACPI is implemented. The total simulation time is calculated as (5.11) and was measured as 46 s. In the second simulation, the macro calculating index ACPI is ignored so that the calculation time of this index is not included in the total simulation time, and can be expressed as follows:

$$Tt=BCT \tag{5.12}$$

The total simulation time of this case was measured as 44s. Thus, BCT and ICT for the case implementing index ACPI can be illustrated as figure 5.14

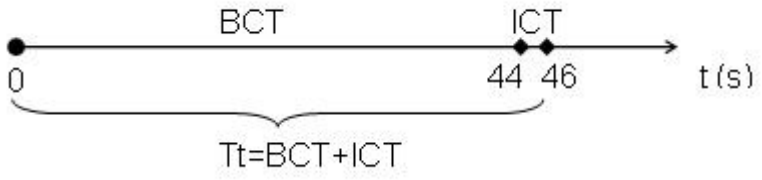

Figure 5.13 Total simulation time and its fractions

Figure 5.14 shows that ICT (2s) is very small compared to BCT (44s). This makes it difficult to compare calculation time of different indices. Besides, it shows that calculation time of the indices are very fast comparing to the total simulation time.

To make the calculation time of the indices comparable, one way is amplifying ICT by K times. This is corresponding to implementing the macros calculating the index (e.g. ACPI_index.mac in figure 5.13) K time repeatedly in each variant calculation. In this test, for each variant calculation, the macro will be calculated repeatedly 500 times. By this approach, the total simulation time of the simulation was measured again for the case implementing the index ACPI. The total simulation time was 325 seconds. Repeating the simulation with different indices to measure the total simulation time corresponding to each index, the results are shown in table 5.15.

	Djj	|Qjj/ej|	VCPI	PTSI	Lmn	ACPI
Tt (s)	144	120	122	145	128	325
Remarks	++	++++	++++	++	+++	+

Table 5.15 Comparison of the calculation time of indices

Table 5.15 shows the index with more '+' is faster to calculate. In the comparison, index |Qjj/ej| is the fastest while index ACPI is the slowest.

5.2.5 Remarks of the larger network test

The larger network tests have shown that:

- It is possible to implement the indices on large networks.
- Index ACPI has better performance than PTSI regarding to sensitivities.
- Calculation time of indices are comparable with the results presented in table 5.15

6 Conclusion

This thesis evaluates the existing Siemens' voltage stability criteria Djj, |Qjj|/ej by comparing its performance with some well-known voltage stability indices including Lmn, VCPI, PTSI, and a new proposed index based on quadratic approximation of PV curves, ACPI. All indices are applied in the reduced local network. The calculation algorithm of these indices in simulation tool PSS®NETOMAC is presented.

The performances of these indices are verified through both steady state and dynamic analysis. They are tested in the 9 bus- 3 generator system, and the more practical, larger network including 414 buses, and 119 generators. It shows that their performances are coherent to each other regarding to voltage stability of the system. All indices fall between 0 and 1. When the system is stable, these indices are closed 0. When the system is more critical, the indices move towards closed to 1, but with different levels of convergence to 1.

The performances of the indices regarding to sensitivity, and calculation time can be summarized as in table 6.1, where more '+' sign indicates better performance.

	Djj	|Qjj/ej|	VCPI	PTSI	Lmn	ACPI
Sensitivity	+	+	+	+++	++	++++
Calculation time	++	++++	++++	++	+++	+

Table 6.1 Comparison of the indices

Table 6.1 shows that Siemens criteria Djj, |Qjj/ej| are less sensitive compared to other indices, however, they have advantages of fast calculation time, especially, index |Qjj/ej|. Index ACPI is the most sensitive one, however, costs more computational time. Since all the indices are very fast to be calculated, index ACPI is highly recommended to be implemented in a voltage assessment module in the power system simulator PSS®NETOMAC

In this thesis, test systems are equipped with AVR and OXL. The loads are modeled as constant power loads. Some indices such as PTSI, ACPI are defined under assumptions that the equivalent voltage of the local network is constant with the variation of load power.

For more intensive study, the system should be modeled more detailed, e.g. with existences of on-load tap changer transformers, and dynamic loads. For more accuracy in calculation of indices PTSI, and ACPI, it is capable to use Thevenin equivalent voltage and impedance viewed from a load bus instead of the local network parameters. Therefore, it is maybe useful to track Thevenin equivalent parameters in the simulation tool PSS®NETOMAC

References

[1] W. Bialek: Cambridge Working Papers in Economics CWPE 0407, 2004

[2] T.V Cutsem: “Voltage stability of electric power system”, Springer, 1998

[3] G.K. Morison: “Voltage stability using static and dynamic approach”, in: IEEE Transaction on Power Systems, Vol. 8, No. 3, August 1993, p. 88-100

[4] J.C. Chow: “On the evaluation of voltage collapse criteria”, in IEE Transaction on Power Systems, Vol. 5, No. 2, May 1990, p. 612-620

[5] P.A. Lof: “Voltage stability indices for stressed power systems”, in IEEE Transaction on Power Systems, Vol. 8, No. 1, February 1993, p. 326-335

[6] B. Gao: “Voltage stability evaluation using modal analysis”, in Transactions on Power Systems, Vol. 7, No. 4, November 1992, p. 1529-1542

[7] B. Lee: “Invariant subspace parametric sensitivity (ISPS) of structure-preserving power system models”, IEEE Transaction on Power System, Vol.11, No.2, May 1996, p. 845-850

[8] P. Kessel: “Estimating the voltage stability of a power system”, in IEEE Transaction on Power Delivery, Vol. PWRD-1, No. 3, July 1986, p. 346-354

[9] M. Moghavemi: “Real-time contingency evaluation and ranking technique”, in IEE Procedure on Generation, Transmission and Distribution, Vol. 145, No. 5, September 1998, p. 517-524

[10] V. Balamourougan: “Technique for online prediction of voltage collapse”, in IEE Procedure on Generation, Transmission and Distribution, Vol.151, No. 4, July 2004, p. 453-460

[11] M.H. Haque: “On-line monitoring of maximum permissible loading of a power system within voltage stability limits”, in IEE Procedure on Generation, Transmission and Distribution, Vol. 150, No. 1, January 2003, p. 107-112

[12] P. Kundur: “Definition and classification of power system stability”, in IEEE Transaction on Power Systems, Vol.19, No. 2, May 20004, p. 1387-1401

[13] P. Kundur: “Power system stability and control”, McGraw-Hill, Inc, Palo Alto, California, 1994

[14] O. Ruhle: “PSS®NETOMAC application guilde”, Siemens AG, PTD PTI SE, 2003

[15] C.A. Canizares: “Basic theoretical concept, Chapter 5 Voltage stability indices”, in IEEE Power Engineering Society, August 2004

[16] N. Flatabo: “Voltage stability condition in a power transmission system calculated by sensitivity methods”, in IEEE Transaction on Power Systems, Vol. 5, No. 4, November 1990, p.1286-1295

[17] F. Gubina: “Voltage collapse proximity index determination using voltage phasor approach”, in IEEE Transaction on Power Systems, Vol. 10, No. 2, p. 788-794

[18] M. Nizam: “Estimating the voltage stability of a power system”, in IEEE Transaction on Power Delivery, Vol. PWRD-1, No. 3, July1986, p. 346-354

[19] T. An: “Research on illed-condition equations in tracking Thevenin equivalent parameters with local measurement’’, International Conference on Power System Technology, 2006

[20] K. Vu: “Use of local measurements to estimate voltage stability margin’’, in IEEE Transaction on Power System, Vol. 14, No. 3, August 1999, p. 1029-1235

[21] Z. Wang: “Master thesis: Investigation of voltage stability criteria to be used in DAS system’’, RWTH Aachen University, 2009

[22] A. Pama: “A new approach for estimating voltage collapse point based on quadratic approximation of PV-curves’’, in Electric Power System Research 79, 2009, p. 653-659

[23] “IEEE Recommended Practice for Excitation System Models for Power System Stability Studies’’, IEEE Power Engineering Society, New York, April 2006.

Appendix

Appendix 1 Calculate the first-order and second- order derivative $dV_i / d\lambda_i$ and $d^2V_i / d\lambda_i^2$

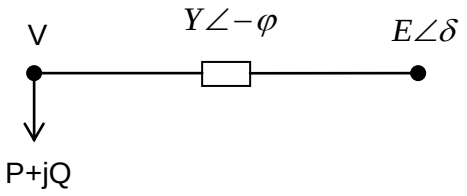

Figure A.1 The reduced local network

Figure A1 illustrates a reduced local network viewed from a load bus. Power flow equations written at the node are as follows:

$$P = P_0(1+d\lambda) = YEV\sin(\delta+\gamma) - YV^2\sin(\gamma) \quad \text{(A1.1)}$$

$$Q = P_0(1+q\lambda) = YEV\cos(\delta+\gamma) - YV^2\cos(\gamma) \quad \text{(A1.2)}$$

Where P, Q, and V are the powers, and voltage magnitude at the load bus

$E\angle\delta, Y\angle -\varphi$ are the equivalent voltage and self admittance of the local network viewed from the load bus; $\gamma = 90 - \varphi$

Assuming that the equivalent voltage E is constant, taking the first order derivative of (A1.1) and (A1.2) to λ gives:

$$\frac{dP}{d\lambda} = P_0 d = YEV\cos(\delta+\gamma)\frac{d\delta}{d\lambda} + [YE\sin(\delta+\gamma) - 2YV\sin\gamma]\frac{dV}{d\lambda} \quad \text{(A1.3)}$$

$$\frac{dQ}{d\lambda} = Q_0 q = -YEV\sin(\delta+\gamma)\frac{d\delta}{d\lambda} + [YE\cos(\delta+\gamma) - 2YV\cos\gamma]\frac{dV}{d\lambda} \quad \text{(A1.4)}$$

Solving equations (A1.3), (A1.4) for the first order derivatives $d\delta / d\lambda$, and $dV / d\lambda$ gives:

$$\frac{d\delta}{d\lambda} = \frac{[E\cos(\delta+\gamma) - 2V\cos\gamma]dP_0 - [E\sin(\delta+\gamma) - 2V\sin\gamma]qQ_0]}{YEV(E - 2V\cos\delta)} \quad \text{(A1.5)}$$

$$\frac{dV}{d\lambda} = \frac{\sin(\delta+\gamma)dP_0 + \cos(\delta+\gamma)qQ_0}{Y(E - 2V\cos\delta)} \quad \text{(A1.6)}$$

The second derivative of V to λ is calculated from partial derivatives as follows:

$$\frac{d^2V}{d\lambda^2} = \frac{\partial}{\partial\delta}\left(\frac{dV}{d\lambda}\right)\frac{d\delta}{d\lambda} + \frac{\partial}{\partial V}\left(\frac{dV}{d\lambda}\right)\frac{dV}{d\lambda} \quad \text{(A1.7)}$$

Taking derivative both sides of equation (A1.6) to δ give:

$$\frac{\partial}{\partial\delta}\left(\frac{dV}{d\lambda}\right) = \frac{E[\cos(\delta+\gamma)dP_0 - \sin(\delta+y)qQ_0] - 2V(\cos\delta dP_0 - \sin\gamma qQ_0)}{Y(E - 2V\cos\delta)^2} \quad \text{(A1.8)}$$

Similarly, $\frac{\partial}{\partial V}\left(\frac{dV}{d\lambda}\right)$ is obtained by taking derivative both sides of equation (A1.6) to V:

$$\frac{\partial}{\partial V}\left(\frac{dV}{d\lambda}\right) = \frac{2\cos\delta[\sin(\delta+\gamma)dP_0 + \cos(\delta+y)qQ_0]}{Y(E - 2V\cos\delta)^2} \quad \text{(A1.9)}$$

Finally, the second derivative of V to λ is calculated by inserting (A1.5) (A1.6), and (A1.8), (A1.9) into (A1.7)

Appendix 2 9 bus- 3 generator test system parameters

- Synchronous machine parameters are listed in table A.1.
- Transmission line and transformer parameters are listed in table A.2 and A.3
- Figure A.1 shows the exciter control diagram. The parameters setting for each generator's exciter are shown in table A.4 and A.5

Parameter	Unit	Gen1	Gen2	Gen3
Rated power, S	MVA	247.5	192	128
Rated voltage, V	kV	16.5	18	13.8
Rated power factor, $\cos\varphi$		0.9	0.85	0.85
Rated frequency, f	Hz	60	60	60
Starting time, TA	s	19.1	6.667	128
Armature resistance	pu	1.E-6	1.E-6	1.E-6
Armature leakage reactance	pu	0.08316	0.102	0.095
Sub-transient time d-axis	s	1.E-6	0.033	0.034
Sub-transient reactance d-axis	pu	0.1505	0.171	0.171
Transient reactance d-axis	pu	0.1505	0.232	0.232
Synchronous reactance d-axis	pu	0.3613	1.651	1.68
Sub-transient time q-axis	s	1.E-6	0.078	0.080
Sub-transient reactance q-axis	pu	0.2395	0.171	0.171
Transient time q-axis	s	1.E-6	0.535	0.600
Transient reactance q-axis	pu	0.2395	0.38	0.32
Synchronous reactance q-axis	pu	0.2395	1.59	1.610

Table A.1 Synchronous machine parameters

Line	L [km]	R [Ω/km]	X [Ω/km]	V [kV]
B4-B5	55	0.055	0.544	230
B5-B7	45	0.071	0.724	230
B7-B8	35	0.055	0.544	230
B8-B9	55	0.055	0.544	230
B9-B6	45	0.071	0.724	230
B6-B4	45	0.071	0.724	230

Table A.2 Transmission line parameters

Parameter	Unit	T1	T2	T3
Rated power	MVA	247.5	192	128
Connection		Yy	Yy	Yy
Rated high voltage side	kV	230	230	230
Rated low voltage side	kV	16.5	18	13.8
Short circuit voltage	%	12	8	8

Table A.3 Transformer parameters

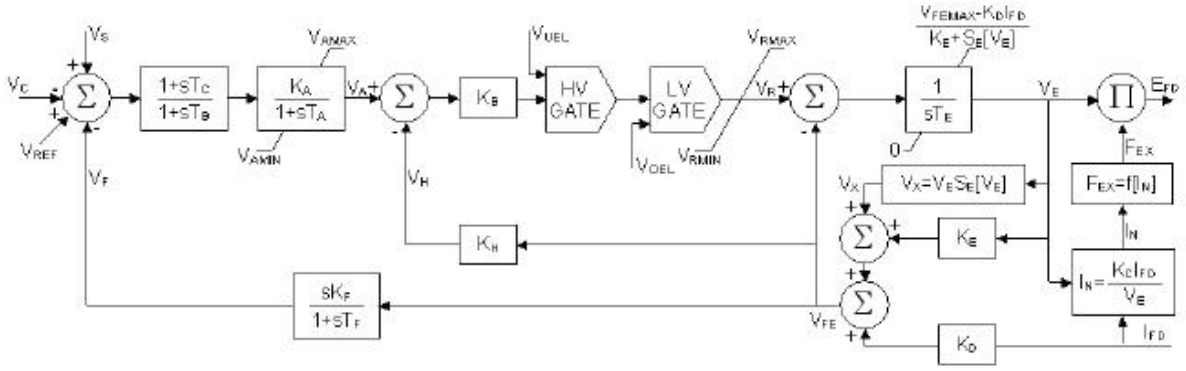

Figure A.2 Excitation system type AC2A- [23]

Parameter	Gen1	Gen2	Gen3	Comment
XDU	0.3613	1.651	1.68	Unsaturated Xd [pu] of the generator
XL	0.08316	0.102	0.095	Armature leakage reactance Xl [pu] of the generator

Table A.4 Parameter setting of exciter type IEEE CA2A (a)

Parameter	Setting value	Comment
XDU	2.19	Unsaturated Xd [pu] of the generator
XL	0.156	Armature leakage reactance Xl [pu] of the generator
TR	0.02	Measuring time constant TR [s]
VAMAX1	20.93	AVR-limit VAmax1 [non-reciprocal pu of EFD]
VAMAX2	28.43	AVR-limit VAmax2 [non-reciprocal pu of EFD]
VAMIN1	0	AVR-limit VAmin1 [non-reciprocal pu of EFD]
VAMIN2	-28.43	AVR-limit VAmin2 [non-reciprocal pu of EFD]
VRMAX	70.31	CR-limit VRmax [non-reciprocal pu of EFD]
VRMIN1	-70.31	CR-limit VRmin1 [non-reciprocal pu of EFD]

VRmin2	0	CR-limit VRmin2 [non-reciprocal pu of EFD]
KA	50	AVR gain KA [s]
TA	0.001	AVR time constant TA [s]
KB	2	CR gain KB [non-reciprocal pu of EFD]
TB	0.2	CR time constant TB [s]
KH	1.0	CR feedback KH[non-reciprocal pu of EFD]
KF	0.01	Time constant (differentiation) KF [s]
TF	0.50	Time constant TF [s]
KD	3.60	Armature reaction KD of exciter [non-reciprocal pu of EFD]
TE	1.70	Time constant TE [s] of exciter's field winding
EFD1	14.79	Value of EFD1 at saturation begin [non-reciprocal pu of EFD]
SE1	0	Saturation of IFE at VE=VE1 [non-reciprocal pu of EFD]
EFD2	13.17	Value of EFD2 at saturation end [non-reciprocal pu of EFD]
SE2	0	Saturation of IFE at VE=VE2< VE1 [non-reciprocal pu of EFD]

Table A.5 Parameter setting of exciter type IEEE CA2A (b)

Appendix 3 Larger test network

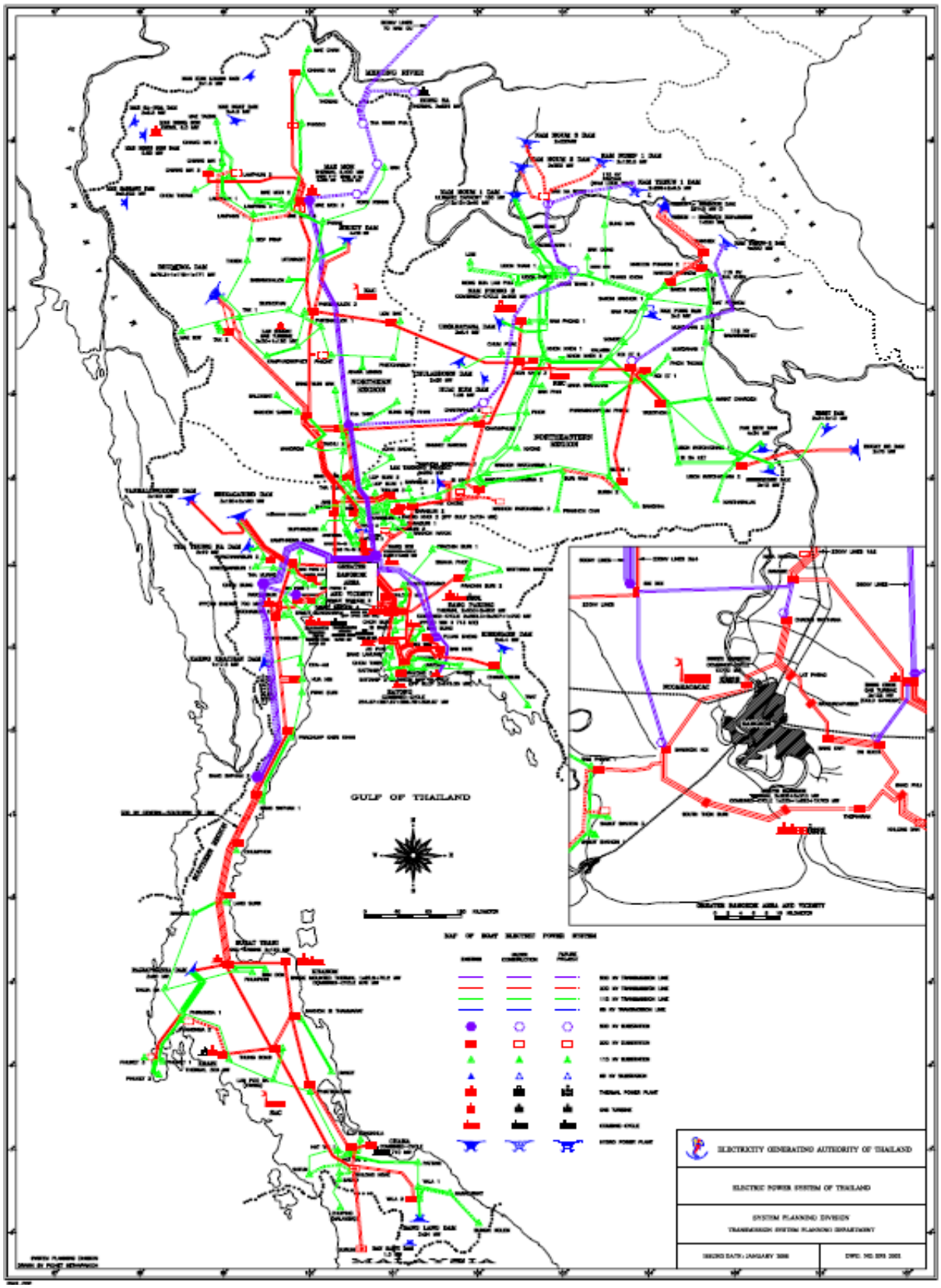

Figure A.3 Larger test network overview [21]

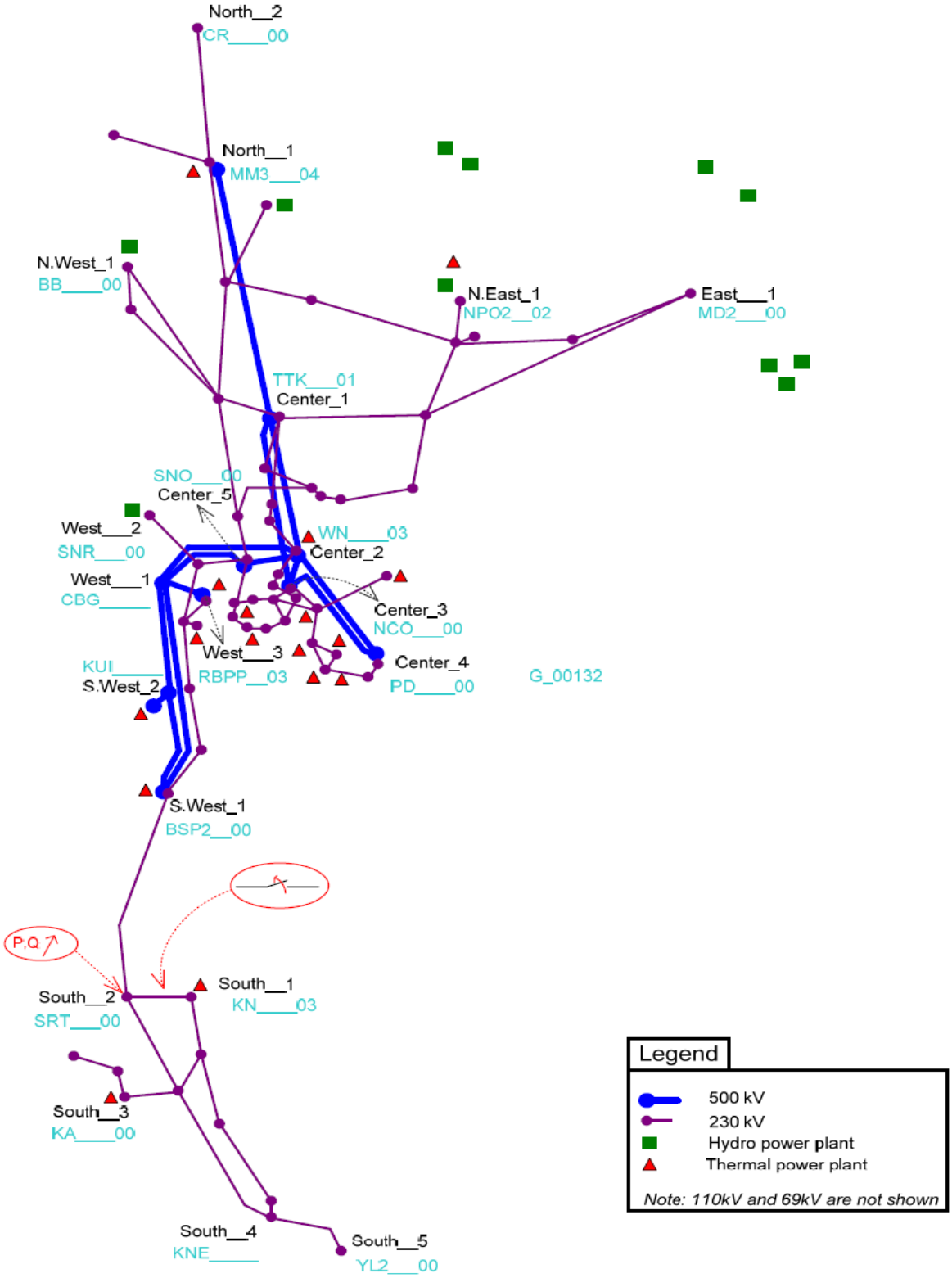

Figure A.4 Contingency locations [21]

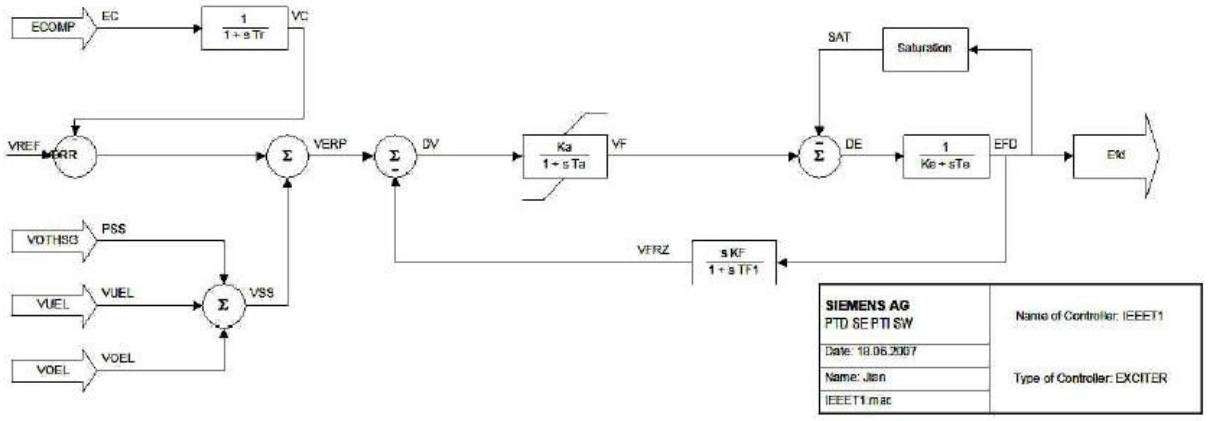

a)

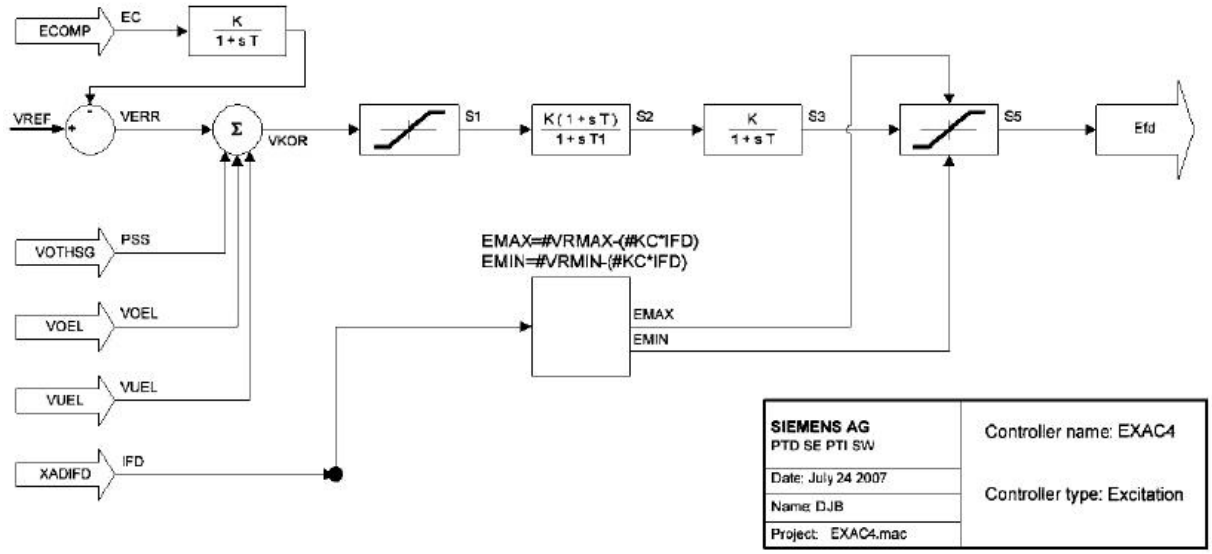

b)

ccc

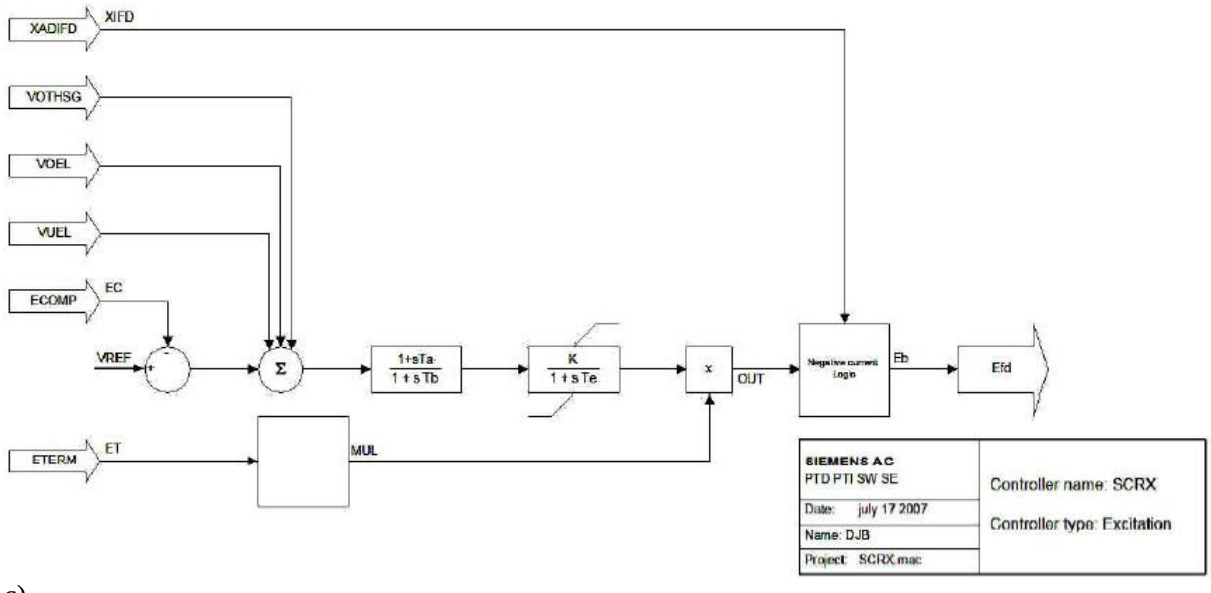

c)

Figure A.5 Block diagrams of AVRs used in the larger test network [21]

```
$-------------------------------------------------------------------------------
$                Parameter setting of Auto Voltage Regulators
$-------------------------------------------------------------------------------
$                                 Type 1: IEEET1
$-------------------------------------------------------------------------------
@#NAME='G_00001', #cosfi=7.292E-001, #GKnot='NB____T1', #XHD=1.872E+000
$ EXITATION SYSTEM DATA: (IEEET1    , 11001)
@#TR=0.000E+000, #KA=0.900E+002, #TA=2.000E-002, #VRMAX=7.300E+000
@#VRMIN=-7.300E+000, #Ke=1.000E+000, #Te=8.000E-001, #KF=3.000E-002
@#TF=1.000E+000, #XXX=0.000E+000, #Sx1=2.900E+000, #Sy1=5.000E-001
@#Sx2=3.900E+000, #Sy2=8.600E-001
GIEEET1  STANDARD
...
...
$-------------------------------------------------------------------------------
$                                 Type 2: SCRX
$-------------------------------------------------------------------------------
@#NAME='G_00160', #cosfi=8.537E-001, #GKnot='TECO__T1', #XHD=1.700E+000
$ EXITATION SYSTEM DATA: (SCRX     , 74003)
@#TA_TB=1.500E-001, #TB=1.000E+001, #K=1.000E+002, #TE=4.000E-002
@#EMIN=0.000E+000, #EMAX=4.000E+000, #CSWITCH=0.000E+000, #RC_RFD=0.000E+000
$ PSS DATA: (IEEEST   , 74003)
@#ACTy=1.0
@#Jy=3.000E+000, #Ky=0.000E+000, #A1y=0.000E+000, #A2y=0.000E+000
@#A3y=0.000E+000, #A4y=0.000E+000, #A5y=0.000E+000, #A6y=0.000E+000
@#T1y=6.000E-002, #T2y=1.800E-001, #T3y=6.000E-002, #T4y=1.800E-001
@#T5y=5.000E+000, #T6y=5.000E+000, #KSy=-7.500E-001, #LSMAy=1.000E-001
@#LSMIy=-1.000E-001, #VCUy=0.000E+000, #VCLy=0.000E+000, #VPSS=1.000E+000
GSCRX    STANDARD
...
...
$-------------------------------------------------------------------------------
$                                 Type 3: EXAC4
$-------------------------------------------------------------------------------
@#NAME='G_00098', #cosfi=4.938E-001, #GKnot='BPK___C1', #XHD=2.160E+000
$ EXITATION SYSTEM DATA: (EXAC4    , 61001)
@#TR=0.000E+000, #VIMAX=2.000E-001, #VIMIN=-2.000E-001, #TC=1.500E+000
@#TB=1.000E+001, #KA=0.900E+002, #TA=4.000E-002, #VRMAX=4.000E+000
@#VRMIN=0.000E+000, #KC=0.000E+000
GEXAC4   STANDARD
...
...
$-------------------------------------------------------------------------------
```

Figure A.6 Parameter setting of AVRs used in the larger test network [21]

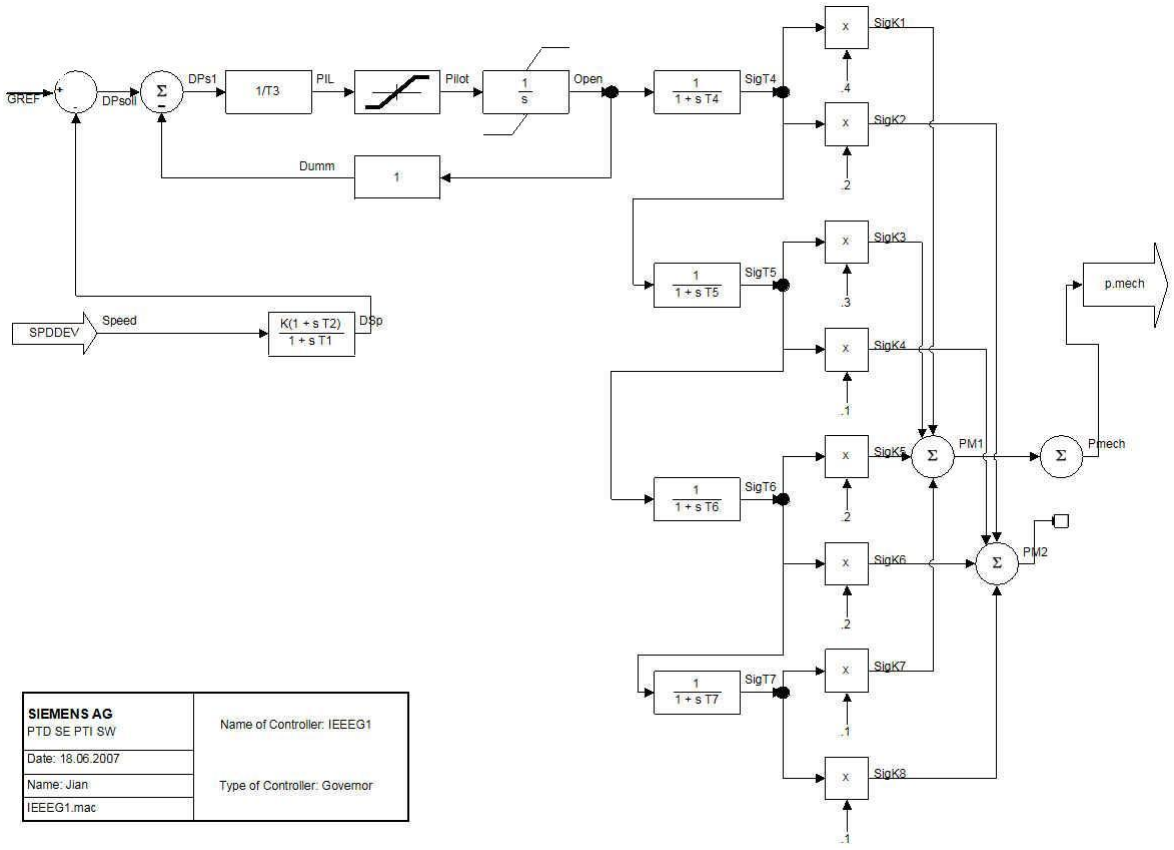

a)

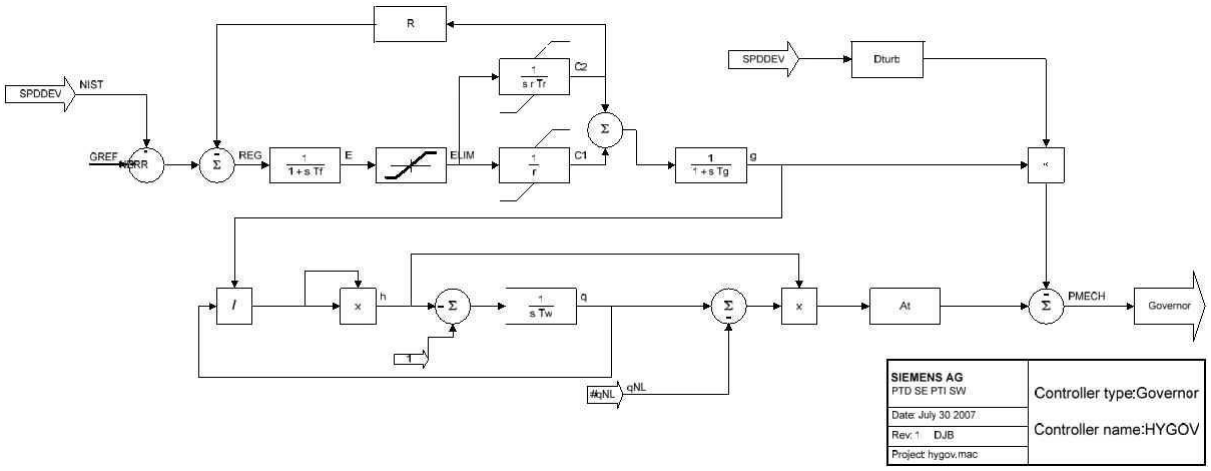

b)

Figure A.7 Block diagrams of governors used in the larger test network [21]

```
$-------------------------------------------------------------------------------|
$                          Parameter setting of Speed Governors                 |
$-------------------------------------------------------------------------------|
$                          Type 1: IEEEG1                                       |
$-------------------------------------------------------------------------------|
@#NAME='G_00149', #cosfi=8.485E-001                                             |
$ TURBINE GOVERNOR: (IEEEG1    , 71015)                                         |
@#J=0.000E+000, #JM=0.000E+000, #K=2.000E+001, #T1=2.500E-001                   |
@#T2=0.000E+000, #T3=1.000E-001, #UO=1.000E-001, #UC=-1.000E-001                |
@#PMAX=1.000E+000, #PMIN=0.000E+000, #T4=3.000E-001, #K1=3.000E-001             |
@#K2=0.000E+000, #T5=1.000E+001, #K3=4.000E-001, #K4=0.000E+000                 |
@#T6=4.000E-001, #K5=3.000E-001, #K6=0.000E+000, #T7=0.000E+000                 |
@#K7=0.000E+000, #K8=0.000E+000                                                 |
GIEEEG1  STANDARD                                                               |
$-------------------------------------------------------------------------------|
$                          Type 2: HYGOV                                        |
$-------------------------------------------------------------------------------|
@#NAME='G_00170', #cosfi=7.937E-001                                             |
$ TURBINE GOVERNOR: (HYGOV     , 86022)                                         |
@#R1=4.000E-002, #R2=3.500E-001, #TR=6.500E+000, #TF=5.000E-002                 |
@#TG=2.000E-001, #VELM=8.300E-002, #GMAX=1.000E+000, #GMIN=0.000E+000           |
@#TW=2.210E+000, #AT=1.110E+000, #DTURB=5.000E-001, #QNL=1.000E-001             |
GHYGOV   STANDARD                                                               |
$-------------------------------------------------------------------------------|
```

Figure A.8 Parameter setting of governors used in the larger test network [21]

Appendix 4 Variations of total simulation time (Tt) to integration time step (dt) and number of contingencies (Nc)

To show the relation between total calculation time (Tt) to integration time step (dt), 60 variants of branch contingencies are applied in the larger test network where index ACPI is calculated at node SRT___00. The simulation time of each variant calculation Tsim is 50s. The total calculation time is counted from starting the simulation until the last results are achieved. For each dt, different Tt are obtained as shown in figure A.9

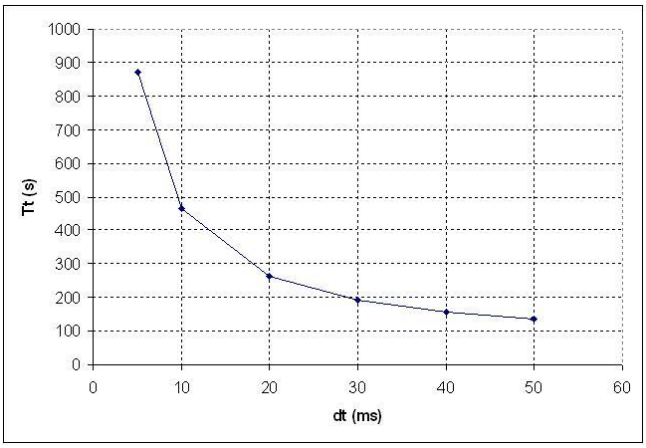

Figure A.9 Variation of the total simulation time to integration time step

From figure A.9, it shows that when the integration time step decreases, total calculation time increases.

The total calculation time also depend on the number of contingencies analyzed, or number of variant calculations. To show the relation between the total simulation time and the number of contingencies (Nc), integration time step is selected as 20 ms, and simulation time of each variant is Tsim equal 50s. For the simulation where index ACPI is calculated, with each Nc, Tt is counted and illustrated in figure A.10

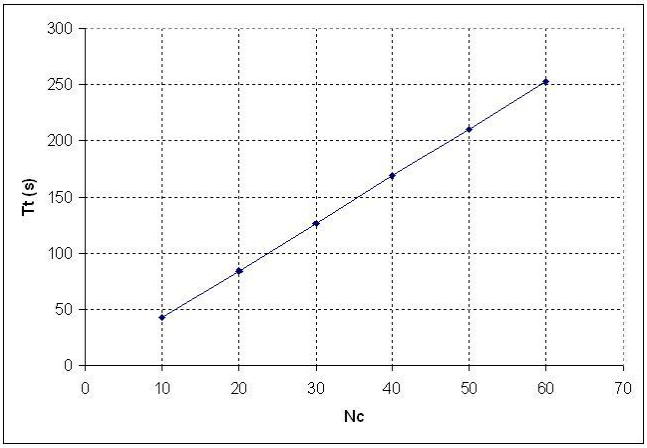

Figure A.10 Variation of the total simulation time to the number of contingencies

From figure 5.10, it shows that Tc is proportional to Nc

Appendix 5 Some macros used in the larger test network

```
$-------------------------------------------------------------------------------|
$1111111122222223333333AA1111112222223333334444445555556666667777788888999999ZZ|
 EVALUATE          #BR       N                                                  |
$-------------------------------------------------------------------------------|
 ANGV1             INPUT      1.                 020000                        |
W#node1                      R                                                 |
 AV1      ANGV1    ANGLE                                                       |
 MV1               INPUT      1.                 020000                        |
B#node1                      R                                                 |
$-------------------------------------------------------------------------------|
 ANGV2             INPUT      1.                 020000                        |
W#node2                      R                                                 |
 AV2      ANGV2    ANGLE                                                       |
 MV2               INPUT      1.                 020000                        |
B#node2                      R                                                 |
$-------------------------------------------------------------------------------|
 ANGI12            INPUT      1.                 020000                        |
W                  #BR                                                         |
 AI12     ANGI12   ANGLE                                                       |
 MI12              INPUT      1.                 020000                        |
B                  #BR                                                         |
$-------------------------------------------------------------------------------|
 V1                AA/RI                         MV1    AV1                    |
 V2                AA/RI                         MV2    AV2                    |
 RDV12=V1-V2                                                                   |
 IDV12=V1.1-V2.1                                                               |
 DV12              RI/AA                         RDV12  IDV12                  |
 MY12=MI12/DV12                                                                |
 AY12=AI12-DV12.1                                                              |
 Y12               AA/RI                         MY12   AY12                   |
 RY12=Y12                                                                      |
 IY12=Y12.1                                                                    |
                   ENDE                                                        |
$1111111122222223333333AA1111112222223333334444445555556666667777788888999999ZZ|
```

Figure A.11 Macro calculating branch admittance Yij.mac

```
$-------------------------------------------------------------------------------|
@@ #node0='MM3___T8'                                                            |
@@ #node1='KN____03', #BR1='L_00239', #BR2='L_00240'                            |
@@ #node2='RPB___00', #BR3='L_00251', #BR4='L_00252'                            |
@@ #node3='TS____00', #BR5='L_00253', #BR6='L_00254'                            |
@@ #node4='BSP___00', #BR7='L_00255', #BR8='L_00256'                            |
@@ #node5='SRT_____', #BR9='T_00098', #BR10='T_00099',#BR11='T_00100'           |
@@ #nodej='SRT___00', #BRj='Load_SRT'                                           |
@#nodeA='KN____03', #nodeB='SRT___00', #BR=#BR1                                 |
#Yij.mac                                                                        |
@#nodeA='KN____03', #nodeB='SRT___00', #BR=#BR2                                 |
#Yij.mac                                                                        |
@#nodeA='RPB___00', #nodeB='SRT___00', #BR=#BR3                                 |
#Yij.mac                                                                        |
@#nodeA='RPB___00', #nodeB='SRT___00', #BR=#BR4                                 |
#Yij.mac                                                                        |
@#nodeA='SRT___00', #nodeB='TS____00', #BR=#BR5                                 |
#Yij.mac                                                                        |
@#nodeA='SRT___00', #nodeB='TS____00', #BR=#BR6                                 |
#Yij.mac                                                                        |
@#nodeA='SRT___00', #nodeB='BSP___00', #BR=#BR7                                 |
#Yij.mac                                                                        |
@#nodeA='SRT___00', #nodeB='BSP___00', #BR=#BR8                                 |
#Yij.mac                                                                        |
@#nodeA='SRT___00', #nodeB='SRT_____', #BR=#BR9                                 |
#Yij.mac                                                                        |
@#nodeA='SRT___00', #nodeB='SRT_____', #BR=#BR10                                |
#Yij.mac                                                                        |
@#nodeA='SRT___00', #nodeB='SRT_____', #BR=#BR11                                |
#Yij.mac                                                                        |
$1111111122222222333333334A1111112222223333334444445555556666667777788888999999ZZ|
 EVALUATE        Yjj      N                                                     |
$-------------------------------------------------------------------------------|
 RYj11           INPUT                        RY12        1                     |
 EVALUATE        #BR1                                                           |
 IYj11           INPUT                        IY12        1                     |
 EVALUATE        #BR1                                                           |
$-------------------------------------------------------------------------------|
```

Figure A.12 Macro calculating the self admittance Yjj.mac (cont)

```
$-------------------------------------------------------------------------------|
 RYj12           INPUT                          RY12        1                    |
 EVALUATE        #BR2                                                            |
 IYj12           INPUT                          IY12        1                    |
 EVALUATE        #BR2                                                            |
$-------------------------------------------------------------------------------|
 RYj21           INPUT                          RY12        1                    |
 EVALUATE        #BR3                                                            |
 IYj21           INPUT                          IY12        1                    |
 EVALUATE        #BR3                                                            |
$-------------------------------------------------------------------------------|
 RYj22           INPUT                          RY12        1                    |
 EVALUATE        #BR4                                                            |
 IYj22           INPUT                          IY12        1                    |
 EVALUATE        #BR4                                                            |
$-------------------------------------------------------------------------------|
 RYj31           INPUT                          RY12        1                    |
 EVALUATE        #BR5                                                            |
 IYj31           INPUT                          IY12        1                    |
 EVALUATE        #BR5                                                            |
$-------------------------------------------------------------------------------|
 RYj32           INPUT                          RY12        1                    |
 EVALUATE        #BR6                                                            |
 IYj32           INPUT                          IY12        1                    |
 EVALUATE        #BR6                                                            |
$-------------------------------------------------------------------------------|
 RYj41           INPUT                          RY12        1                    |
 EVALUATE        #BR7                                                            |
 IYj41           INPUT                          IY12        1                    |
 EVALUATE        #BR7                                                            |
$-------------------------------------------------------------------------------|
 RYj42           INPUT                          RY12        1                    |
 EVALUATE        #BR8                                                            |
 IYj42           INPUT                          IY12        1                    |
 EVALUATE        #BR8                                                            |
$-------------------------------------------------------------------------------|
 RYj51           INPUT                          RY12        1                    |
 EVALUATE        #BR9                                                            |
 IYj51           INPUT                          IY12        1                    |
 EVALUATE        #BR9                                                            |
$-------------------------------------------------------------------------------|
 RYj52           INPUT                          RY12        1                    |
 EVALUATE        #BR10                                                           |
 IYj52           INPUT                          IY12        1                    |
 EVALUATE        #BR10                                                           |
$-------------------------------------------------------------------------------|
 RYj53           INPUT                          RY12        1                    |
 EVALUATE        #BR11                                                           |
 IYj53           INPUT                          IY12        1                    |
 EVALUATE        #BR11                                                           |
$-------------------------------------------------------------------------------|
 RYjj=RYj11+RYj12+RYj21+RYj22+RYj31+RYj32+RYj41+RYj42+RYj51+RYj52+RYj53          |
 IYjj=IYj11+IYj12+IYj21+IYj22+IYj31+IYj32+IYj41+IYj42+IYj51+IYj52+IYj53         |
 Yjj             RI/AA                          RYjj  IYjj                     |
 MYjj=Yjj                                                                      |
 AYjj=Yjj.1                                                                    |
                 ENDE                                                          |
$1.....12.....23.....3AA1....12....23....34....45....56....67...78...89...9ZZ|
```

Figure A.13 Macro calculating the self admittance Yjj.mac

```
$1111111122222222333333334A1111112222223333334444445555556666667777788888999999ZZ
 EVALUATE          #nodej.D N
$-------------------------------------------------------------------------------
$Admitance--------------------------------------------------------------------
 MYjj              INPUT                       MYjj          1
 EVALUATE          Yjj
 AYjj              INPUT                       AYjj          1
 EVALUATE          Yjj
$Equivalent voltage Ej--------------------------------------------------------
 Ej                INPUT                       Ej            1
 EVALUATE          Ej
 AEj               INPUT                       AEj           1
 EVALUATE          Ej
$Reference bus----------------------------------------------------------------
 ANGV0             INPUT      1.               020000
W#node0                      R
 A0       ANGV0    ANGLE
$Bus j------------------------------------------------------------------------
 ANGVj             INPUT      1.               020000
W#nodej                      R
 Aj       ANGVj    ANGLE
 AVj=Aj-A0
 MVj               INPUT      1.               020000
B#nodej                      R
$Power
 Pj                INPUT      1.               020000
P#nodej           #BRj
 Qj                INPUT      1.               020000
Q#nodej           #BRj
$-------------------------------------------------------------------------------
$ej,Pjj,Qjj,Djj,|Qjj|/ej------------------------------------------------------
 ej=MVj/Ej
 delta=AEj-AVj
 Pjj=ej^2-ej*COS(delta)
 Qjj=-1*ej*SIN(delta)
 Djj= 4*(Pjj^2+Qjj^2)/(1+2*Pjj)^2
                   ENDE
$1......12......23......3AA1....12....23....34....45....56....67...78...89...9ZZ
$-------------------------------------------------------------------------------
$<<<<<<<<<<<<<<<<<<<<<<<<<<<<<<<<<<<<<<<<<<<<<<<<<<<<<<<<<<<<<<<<<<<<<<<<<<<<<<
$================================================================== END ====$
```

Figure A.14 Macro calculating index Djj Djj_index.mac

Appendix 6 Simulation results in PSS®NETOMAC

Bus	P(MW)	Vj	Djj	Qjj/ej	VCPI	PTSI	Lmn	ACPI
B5	-99.99	0.954	0.005	0.030	0.036	0.107	0.063	0.198
B6	-99.99	0.955	0.006	0.031	0.038	0.112	0.066	0.205
B8	-99.99	0.962	0.003	0.022	0.027	0.080	0.047	0.152

Bus	P(MW)	Vj	Djj	Qjj/ej	VCPI	PTSI	Lmn	ACPI
B5	-199.99	0.921	0.024	0.063	0.078	0.220	0.131	0.355
B6	-100.00	0.946	0.006	0.032	0.039	0.114	0.067	0.208
B8	-100.00	0.953	0.003	0.023	0.027	0.081	0.048	0.155

Bus	P(MW)	Vj	Djj	Qjj/ej	VCPI	PTSI	Lmn	ACPI
B5	-299.97	0.879	0.064	0.101	0.129	0.342	0.207	0.491
B6	-99.99	0.932	0.006	0.033	0.040	0.117	0.069	0.213
B8	-99.99	0.940	0.003	0.023	0.028	0.083	0.049	0.158

Bus	P(MW)	Vj	Djj	Qjj/ej	VCPI	PTSI	Lmn	ACPI
B5	-399.94	0.823	0.142	0.148	0.196	0.481	0.297	0.619
B6	-99.99	0.912	0.007	0.034	0.042	0.122	0.072	0.221
B8	-99.99	0.923	0.003	0.024	0.029	0.086	0.051	0.163

Bus	P(MW)	Vj	Djj	Qjj/ej	VCPI	PTSI	Lmn	ACPI
B5	-499.88	0.736	0.313	0.217	0.306	0.661	0.425	0.759
B6	-99.98	0.878	0.008	0.037	0.045	0.131	0.078	0.235
B8	-99.99	0.896	0.004	0.026	0.031	0.091	0.054	0.172

Bus	P(MW)	Vj	Djj	Qjj/ej	VCPI	PTSI	Lmn	ACPI
B5	-549.78	0.648	0.534	0.286	0.434	0.806	0.546	0.862
B6	-99.98	0.842	0.009	0.040	0.049	0.142	0.084	0.251
B8	-99.98	0.868	0.004	0.027	0.033	0.097	0.057	0.181

Bus	P(MW)	Vj	Djj	Qjj/ej	VCPI	PTSI	Lmn	ACPI
B5	-559.72	0.599	0.666	0.324	0.517	0.872	0.612	0.908
B6	-99.98	0.821	0.010	0.042	0.051	0.149	0.088	0.261
B8	-99.98	0.852	0.005	0.028	0.034	0.101	0.059	0.187

Figure A.15 9 bus network static analysis without considering reactive power limits

Bus	P(MW)	Vj	Djj	Qjj/ej	VCPI	PTSI	Lmn	ACPI
B5	-99.99	0.954	0.005	0.030	0.036	0.107	0.063	0.198
B6	-99.99	0.955	0.006	0.031	0.038	0.112	0.066	0.205
B8	-99.99	0.962	0.003	0.022	0.027	0.080	0.047	0.152

Bus	P(MW)	Vj	Djj	Qjj/ej	VCPI	PTSI	Lmn	ACPI
B5	-199.99	0.920	0.024	0.063	0.078	0.221	0.131	0.356
B6	-100.00	0.943	0.006	0.032	0.039	0.114	0.068	0.209
B8	-100.00	0.950	0.003	0.023	0.027	0.082	0.048	0.155

Bus	P(MW)	Vj	Djj	Qjj/ej	VCPI	PTSI	Lmn	ACPI
B5	-299.89	0.817	0.085	0.116	0.149	0.387	0.235	0.535
B6	-99.97	0.876	0.008	0.037	0.045	0.132	0.078	0.235
B8	-99.97	0.863	0.004	0.028	0.033	0.098	0.058	0.183

Bus	P(MW)	Vj	Djj	Qjj/ej	VCPI	PTSI	Lmn	ACPI
B5	-350.04	0.718	0.183	0.167	0.225	0.534	0.333	0.662
B6	-99.96	0.809	0.011	0.043	0.053	0.153	0.091	0.267
B8	-99.96	0.777	0.007	0.034	0.041	0.120	0.071	0.218

Bus	P(MW)	Vj	Djj	Qjj/ej	VCPI	PTSI	Lmn	ACPI
B5	-359.98	0.681	0.233	0.188	0.257	0.588	0.372	0.705
B6	-99.96	0.783	0.013	0.046	0.056	0.162	0.096	0.280
B8	-99.95	0.744	0.008	0.037	0.045	0.131	0.077	0.233

Bus	P(MW)	Vj	Djj	Qjj/ej	VCPI	PTSI	Lmn	ACPI
B5	-365.10	0.647	0.284	0.207	0.289	0.637	0.407	0.741
B6	-100.10	0.759	0.014	0.049	0.060	0.172	0.102	0.294
B8	-100.03	0.714	0.009	0.040	0.049	0.141	0.084	0.249

Figure A.16 9 bus network static analysis considering reactive power limits

Disconnected line = No

Bus	Vj	Djj	Qjj/ej	VCPI	PTSI	Lmn	ACPI
B5	0.954	0.005	0.030	0.036	0.107	0.063	0.198
B6	0.955	0.006	0.031	0.038	0.112	0.066	0.205
B8	0.962	0.003	0.022	0.027	0.080	0.047	0.152

Disconnected line = LB7-B8

Bus	Vj	Djj	Qjj/ej	VCPI	PTSI	Lmn	ACPI
B5	0.953	0.005	0.030	0.037	0.108	0.063	0.199
B6	0.933	0.006	0.033	0.040	0.117	0.069	0.213
B8	0.904	0.024	0.063	0.078	0.219	0.131	0.354

Disconnected line = LB8-B9

Bus	Vj	Djj	Qjj/ej	VCPI	PTSI	Lmn	ACPI
B5	0.946	0.005	0.031	0.037	0.109	0.064	0.201
B6	0.962	0.006	0.031	0.037	0.110	0.065	0.202
B8	0.935	0.009	0.038	0.046	0.135	0.080	0.240

Disconnected line = LB9-B6

Bus	Vj	Djj	Qjj/ej	VCPI	PTSI	Lmn	ACPI
B5	0.937	0.006	0.031	0.038	0.111	0.066	0.204
B6	0.906	0.028	0.068	0.084	0.235	0.141	0.375
B8	0.964	0.003	0.022	0.027	0.079	0.047	0.152

Disconnected line = LB6-B4

Bus	Vj	Djj	Qjj/ej	VCPI	PTSI	Lmn	ACPI
B5	0.957	0.005	0.030	0.036	0.107	0.063	0.197
B6	0.912	0.027	0.067	0.083	0.232	0.139	0.371
B8	0.950	0.003	0.023	0.027	0.082	0.048	0.156

Disconnected line = LB4-B5

Bus	Vj	Djj	Qjj/ej	VCPI	PTSI	Lmn	ACPI
B5	0.912	0.027	0.067	0.083	0.233	0.139	0.371
B6	0.958	0.006	0.031	0.038	0.111	0.066	0.204
B8	0.947	0.003	0.023	0.028	0.082	0.048	0.156

Disconnected line = LB5-B7

Bus	Vj	Djj	Qjj/ej	VCPI	PTSI	Lmn	ACPI
B5	0.908	0.023	0.062	0.077	0.217	0.129	0.352
B6	0.933	0.006	0.033	0.040	0.117	0.069	0.213
B8	0.960	0.003	0.022	0.027	0.080	0.047	0.153

Figure A.17 9 bus network line contingency analysis

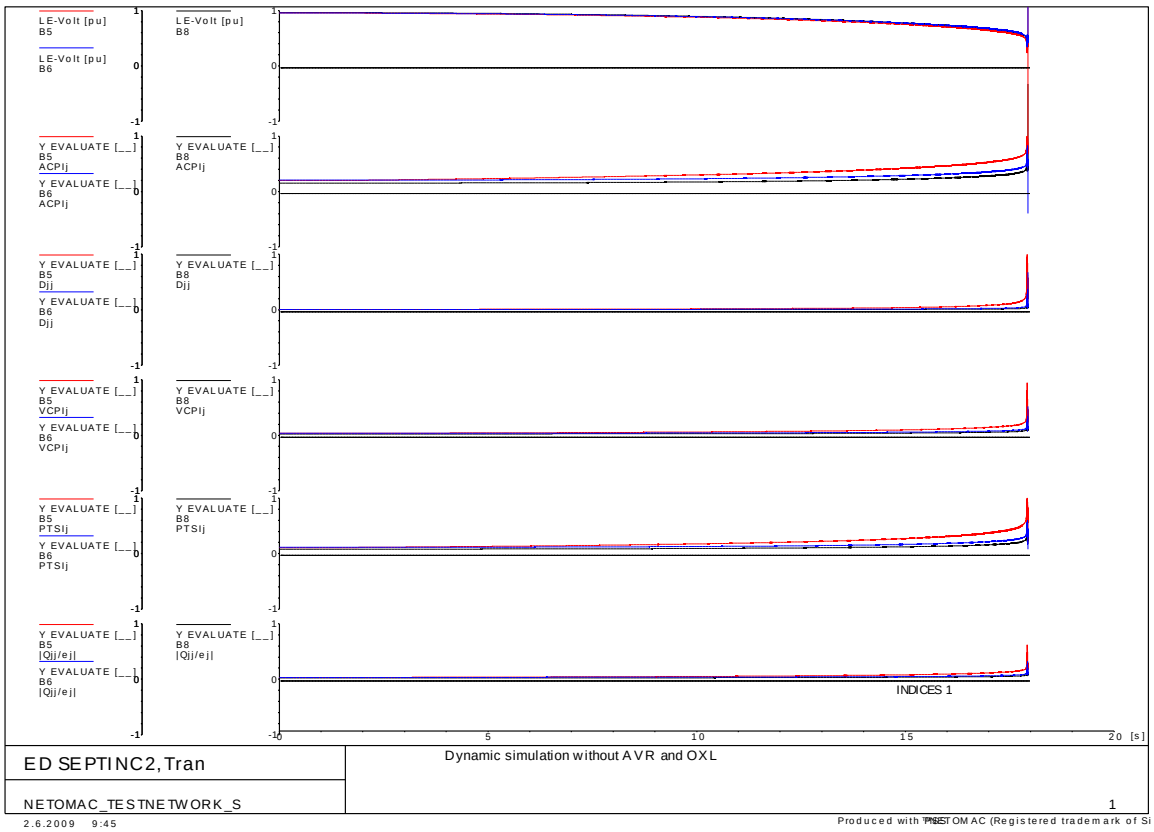

Figure A.18 9 bus network dynamic analysis without considering AVR and OXL

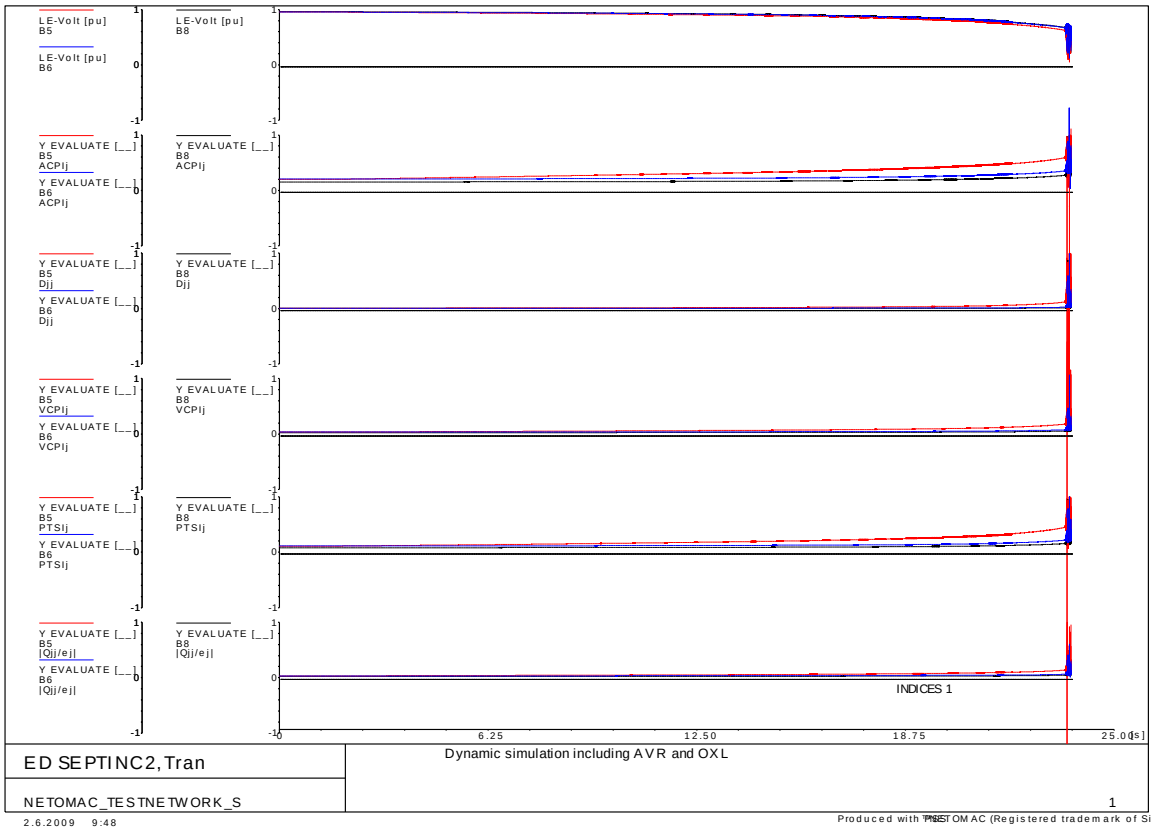

Figure A.19 9 bus network dynamic analysis considering AVR and OXL

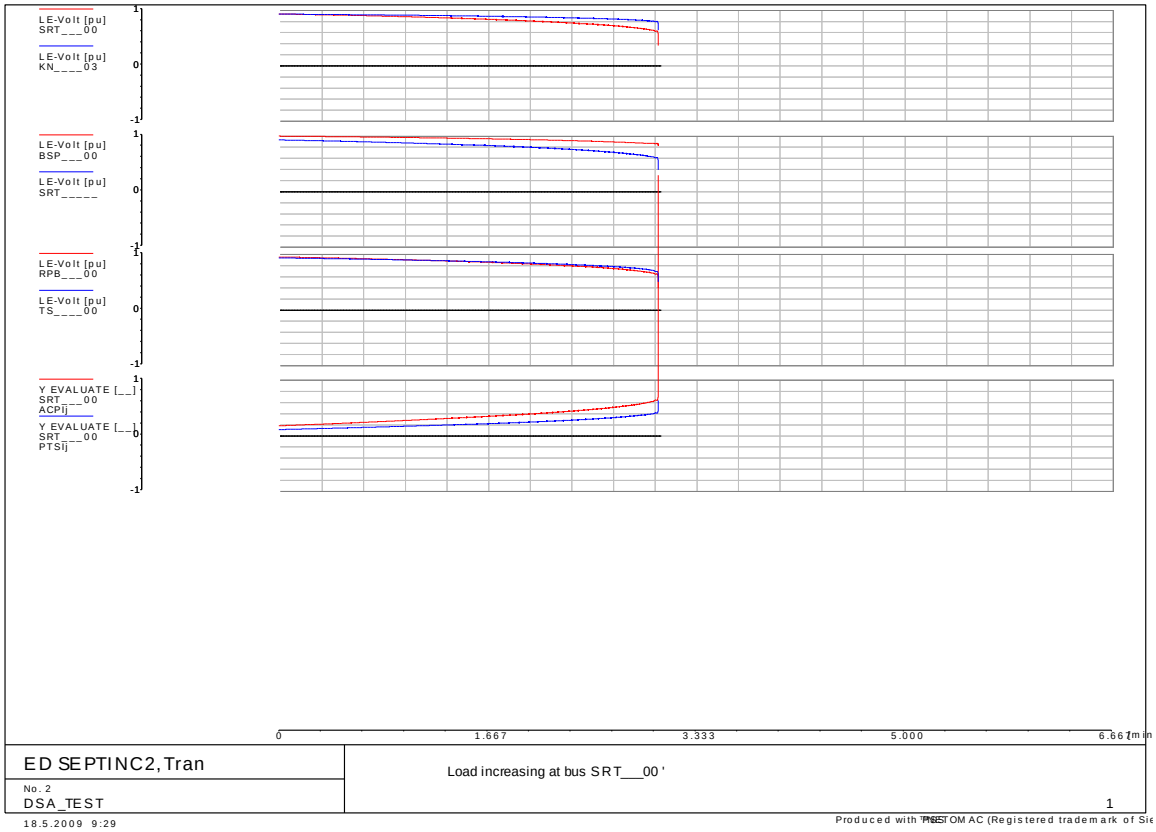

Figure A.20 Larger test network, load increasing at bus SRT___00

Figure A.21 Disconnection of transmission lines in the larger test network